

# On buoyancy in disperse two-phase flow and its impact on well-posedness of two-fluid models

Rui Zhu,<sup>1</sup> Yulan Chen,<sup>1</sup> Katharina Tholen,<sup>2</sup> Zhiguo He,<sup>1†</sup> and Thomas Pätz<sup>1‡</sup>

<sup>1</sup>Institute of Port, Coastal and Offshore Engineering, Ocean College, Zhejiang University, 316021 Zhoushan, China

<sup>2</sup>Institute for Theoretical Physics, Leipzig University, Brüderstraße 16, 04103 Leipzig, Germany

(Received xx; revised xx; accepted xx)

Maxey & Riley's (*Phys. Fluids*, vol. 26, 1983, 883) analytical solution for the flow around a small sphere at low particle Reynolds number tells us that the fluid-particle interaction force decomposes into a contribution from the local flow disturbance caused by the particle's boundary—consisting of the drag, Faxen, virtual-mass, and history forces—and another contribution from the stress of the background flow, termed generalized-buoyancy force. There is also a consensus that, for general disperse two-phase flow, the interfacial force density, resulting from averaging the fluid's and particles' equations of motion, decomposes in a likewise manner. However, there has been a long-standing controversy about the physical closure separating the generalized-buoyancy from the interfacial force density, especially whether or not pseudo-stresses, such as the Reynolds stress, should be attributed to the background flow. Furthermore, most existing propositions for this closure involve small-particle approximations. Here, we show that all existing buoyancy closures are mathematically inconsistent with at least one of three simple thought experiments designed to determine the roles of pseudo-stresses and small-particle approximations. We then derive the unique closure consistent with these thought experiments. It fully incorporates all pseudo-stresses, requires no approximation, and is supported by particle-resolved numerical simulations. Remarkably, it exhibits a low-pass filter property, attenuating buoyancy at short wavelengths, that prevents it from causing Hadamard instabilities, constituting a first-principle-based solution to the long-standing ill-posedness problem of two-fluid models. When employing the derived closure, even very simplistic two-fluid models are hyperbolic.

**Key words:**

## 1. Introduction

Archimedes' principle states that a particle immersed in a stationary fluid experiences a force equal to the negative weight of the fluid it displaces (Batchelor 2000):  $\mathbf{F}_B = - \int_{\mathbb{V}} \rho_f \mathbf{g} dV$ , where  $\rho_f$  is the fluid density,  $\mathbf{g}$  the gravitational acceleration, and  $\mathbb{V}$  the submerged domain

† Email address for correspondence: hezhiguo@zju.edu.cn

‡ Email address for correspondence: 0012136@zju.edu.cn

occupied by the particle. This study addresses the question of how to generalize this so-called buoyancy force to general dynamic fluid-particle systems, where the terms “fluid” and “particle” stand representative for, respectively, a phase of continuous fluid and a dispersed phase consisting of droplets, bubbles, and/or granular particles. Such systems are often modeled by effective two-fluid continuum models, in which buoyancy appears in the form of a generalized-buoyancy force density in the momentum balance equations (e.g., Drew 1983; Stewart & Wendroff 1984; Jackson 2000; Crowe *et al.* 2012; Lhuillier *et al.* 2013; Chauchat 2018). In spite of their widespread use, the partial differential equations (PDEs) underlying such models tend to be ill-posed due to unbounded growth of infinitesimally-small-wavelength perturbations (Stewart & Wendroff 1984; Lhuillier *et al.* 2013; Panicker *et al.* 2018; Langham *et al.* 2025)—a so-called Hadamard instability (Joseph & Saut 1990)—and this buoyancy term has been recognized as the main culprit behind this unphysical behavior (Lhuillier *et al.* 2013). Most of the various solutions proposed to restore hyperbolicity or well-posedness of the PDEs have consisted of introducing into the two-fluid models some kind of buoyancy-unrelated closure relations that dissipate short-wavelength growth contributions (Lhuillier *et al.* 2013; Panicker *et al.* 2018; Zhang 2021; Fox 2019, 2025; Langham *et al.* 2025). However, to our knowledge, no prior study has ever questioned whether the modeling of buoyancy itself may have been the main issue. In the present study, we come to precisely that conclusion, not by design but as a byproduct of a first-principle-based analysis carried out to determine the expression that governs buoyancy in disperse two-phase flow. Our reasoning is built on a careful definition of the term “buoyancy” in dynamic systems, which we introduce below in a manner consistent with known results and common modeling practices.

A sensible definition of a generalized-buoyancy force is obtained from taking a look at a dynamic system that admits an analytical solution for the fluid-particle interaction or hydrodynamic force  $\tilde{\mathbf{F}}_h$ : a single rigid particle submerged in an incompressible Newtonian fluid flow at low particle Reynolds numbers based on the fluid-particle velocity difference and based on the fluid velocity gradient. In this case,  $\tilde{\mathbf{F}}_h$  decomposes into a contribution from the (generally turbulent) undisturbed or background flow, without application of the no-slip boundary conditions at the particle’s surface, and a contribution  $\tilde{\mathbf{F}}_D$  from the disturbance Stokes flow due to the no-slip conditions (Maxey & Riley 1983):

$$\tilde{\mathbf{F}}_h = \int_{\mathbb{V}} \nabla \cdot \tilde{\boldsymbol{\sigma}} dV + \tilde{\mathbf{F}}_D, \quad (1.1)$$

where  $\tilde{\boldsymbol{\sigma}}$  is the instantaneous, local stress tensor of the background flow. With further simplifications—a spherical particle of a radius that is sufficiently smaller than both the distance to the system boundaries and the scale over which the background flow velocity changes— $\tilde{\mathbf{F}}_D$ , which we term generalized-drag force, can be calculated rigorously as the sum of the drag, Faxen, virtual-mass, and history forces; the lift force vanishes (Maxey & Riley 1983). These forces, in addition to the generalized-buoyancy force, are exactly those for which one typically seeks to derive closure expressions applicable to general disperse two-phase flow that does not admit a rigorous solution (Di Felice 1995; Jackson 2000; Loth & Dorgan 2009; Crowe *et al.* 2012; Jamshidi & Mazzei 2018; Shi & Rzehak 2019). Therefore, we interpret the background flow force in (1.1) as the generalized-buoyancy force:

$$\tilde{\mathbf{F}}_B = \int_{\mathbb{V}} \nabla \cdot \tilde{\boldsymbol{\sigma}} dV, \quad (1.2)$$

which is different from the often used pressure ( $\tilde{P}$ )-gradient-based definition  $\mathbf{F}_B = - \int_{\mathbb{V}} \nabla \tilde{P} dV$  (e.g., Drew 1983; Crowe *et al.* 2012; Lhuillier *et al.* 2013; Fox 2019). The latter

is problematic, since it leaves the force  $\int_{\mathbb{V}} \nabla \cdot \tilde{\boldsymbol{\tau}} dV$  due to the instantaneous, local shear stress tensor  $\tilde{\boldsymbol{\tau}} = \tilde{\boldsymbol{\sigma}} + \tilde{P}\mathbf{1}$  of the background flow, where  $\mathbf{1}$  is the identity tensor, as a remainder that is usually not being addressed in two-phase flow closures even though it clearly exists. Using the background flow momentum balance, (1.2) is equivalent to

$$\tilde{\mathbf{F}}_B = \int_{\mathbb{V}} \rho_f (\tilde{D}_t \tilde{\mathbf{u}} - \mathbf{g}) dV, \quad (1.3)$$

where  $\tilde{\mathbf{u}}$  is the instantaneous, local background flow velocity and  $\tilde{D}_t \equiv \partial_t + \tilde{\mathbf{u}} \cdot \nabla$  the associated material derivative, with  $t$  denoting time. Equation (1.3) constitutes a modification of the expression for the stationary case by the term involving  $\tilde{D}_t \tilde{\mathbf{u}}$ , which accounts for fluid inertia and ensures that  $\tilde{\mathbf{F}}_B$  is independent of coordinate transformations into accelerated frames of reference. In particular, for a steady, uniform Stokes flow down a plane inclined by an angle  $\theta$ , (1.3) yields  $\tilde{\mathbf{F}}_B = -\int_{\mathbb{V}} \rho_f \mathbf{g} dV$ , whereas a pressure-gradient-based definition would have resulted in  $\tilde{\mathbf{F}}_B = -\int_{\mathbb{V}} \rho_f \mathbf{g} \cos \theta dV$ , different from the stationary case.

Now, a question that has sparked considerable debate over the past six decades is: What is the background flow stress responsible for buoyancy in general disperse two-phase flow? In other words, what is the analog to  $\tilde{\boldsymbol{\sigma}}$ ? The answer to this question is not trivial, since, when the particle Reynolds numbers are large, nonlinear terms involving the background flow appear in the disturbance flow balance equations, meaning that the background and disturbance flows are no longer decoupled (Maxey & Riley 1983). In addition, closure relations for the generalized-drag force in turbulent particle-laden flows are usually expressed in terms of flow properties that have been averaged in some manner, such as an averaged flow velocity, or whose very existence is tied to some form of averaging, such as the fluid ( $\beta_f$ ) and dispersed-phase ( $\beta_s = 1 - \beta_f$ ) volume fractions (Di Felice 1995; Jackson 2000; Jamshidi & Mazzei 2018). As a consequence, the background flow stress responsible for buoyancy should be somehow related to the averaged flow. However, averaging gives rise to two kind of pseudo-stresses in the fluid phase momentum balance: the Reynolds stress  $\boldsymbol{\sigma}_{\text{Re}}^f$  and a stress due to fluid-particle interactions,  $\boldsymbol{\sigma}_s^f$ , which is responsible for an effective viscosity increase and other effects (Jackson 1997, 2000). This raises the question: Which of these pseudo-stresses should be attributed to the background flow when modeling the generalized-buoyancy force? Anderson & Jackson (1967) proposed that all pseudo-stresses fully contribute to the background flow stress responsible for buoyancy, whereas others considered only the fluid-phase-averaged stress (Zhang *et al.* 2007; Maurin *et al.* 2018). In particular, Maurin *et al.* (2018) argued strongly against including  $\boldsymbol{\sigma}_{\text{Re}}^f$ . Compromises between these two extremes have also been suggested. For example, Chauchat (2018) fully accounted for  $\boldsymbol{\sigma}_s^f$  but disregarded  $\boldsymbol{\sigma}_{\text{Re}}^f$ .

A key problem that has hindered conclusively answering the above question is that it is difficult to empirically test generalized-buoyancy expressions in isolation, since one usually has only access to the total hydrodynamic force or force density. In addition, Reynolds normal stresses tend to be almost negligible relative to the fluid-phase-averaged pressure in unidirectional systems, posing an obstacle to evaluating the effects of  $\boldsymbol{\sigma}_{\text{Re}}^f$  in the gravity-aligned direction where buoyancy effects are usually most important. Lamb *et al.* (2017) are perhaps the only ones who attempted to circumvent these problems. They studied the average total hydrodynamic force acting on objects partially submerged in a shallow turbulent stream down an incline. Their data could be described with a standard drag force closure only if they assumed that the generalized-buoyancy force  $\mathbf{F}_B$  is aligned with the gravity direction, as opposed to the cross-stream direction, implying that  $\mathbf{F}_B$  has a streamwise component and, thus, that the Reynolds shear stress contributes to the background flow shear stress responsible for buoyancy.

Knowing the background flow stress responsible for buoyancy in general disperse two-phase flow is not the end of the story, since integral expressions such as (1.2) can be of limited use and are often approximated as  $\int_V \nabla \cdot \boldsymbol{\sigma}^f dV \approx V \nabla \cdot \boldsymbol{\sigma}^f|_{\mathbf{x}_o}$ , where  $V$  is the particle's volume,  $\mathbf{x}_o$  its center of mass, and  $\boldsymbol{\sigma}^f$  stands as a placeholder for any of the potential background flow stress tensors associated with the average flow. Such kind of approximations, which assume that the particle size is sufficiently small, permit a simple translation of the average generalized-buoyancy force  $\mathbf{F}_B$  acting on a particle into the corresponding interfacial force density  $\beta_s \langle \mathbf{f}_B \rangle^s$  appearing in two-fluid momentum balance equations:  $\beta_s \langle \mathbf{f}_B \rangle^s \approx \beta_s \nabla \cdot \boldsymbol{\sigma}^f$ . However, to the best of our knowledge, the effects of such approximations have not been seriously studied in the literature.

It is also worth noting that some attempts to generalize buoyancy (e.g., Clift *et al.* 1987) were based on expressions analogous to (1.3) rather than (1.2). While the two approaches are equivalent when considering an isolated particle in a pure-fluid flow (i.e.,  $\beta_s \rightarrow 0$ ), they can result in very different outcomes for actual fluid-particle mixture flows, such as homogeneous air-fluidized beds where the effective fluid pressure gradient associated with the fluid-phase-averaged flow supports both the gravitational and generalized-drag force densities. In this case, an expression analogous to (1.3) yields  $\mathbf{F}_B = - \int_V \rho_f \mathbf{g} dV$ , whereas an expression analogous to (1.2) results in  $\mathbf{F}_B = - \int_V \rho_m \mathbf{g} dV$  (Di Felice 1995), where  $\rho_m = \beta_f \rho_f + \beta_s \rho_s \gg \rho_f$  is the mixture density, with  $\rho_s$  the dispersed-phase density. This sparked an intense debate in the 1980s, which was described in some detail by Di Felice (1995). This debate was essentially resolved in favor of expressions involving  $\rho_m$ , and therefore in favor of stress-based expressions analogous to (1.2): It was shown that the hydrodynamic force acting on a coarse particle submerged in an air-fluidized bed of much finer particles can be expressed using a standard but  $\rho_m$ -based closure for the drag force combined with  $\mathbf{F}_B = - \int_V \rho_m \mathbf{g} dV$ , whereas  $\rho_f$ -based approaches fail (Rotondi *et al.* 2015).

Here, we show through two thought experiments—(i) an infinitesimally small neutrally buoyant sphere with free-slip boundary conditions in a statistically steady, uniform turbulent flow and (ii) a statistically steady, uniform particulate Stokes flow of a low but nonzero dispersed-phase volume fraction  $\beta_s$ —that all pseudo-stresses fully contribute to the background flow stress responsible for the generalized-buoyancy force (§2). The only existing closure that satisfies this requirement is the one proposed by Anderson & Jackson (1967). However, we then demonstrate that this and most other closures are inconsistent with a third thought experiment—a particle bed immersed in a fluid at rest with vertically stratified weight density  $\rho_f \mathbf{g}$ —due to small-particle approximations involved in their derivations (§3). To perform this consistency check, we employ mathematically exact micromechanical expressions for the stresses appearing in the fluid phase momentum balance, derived from averaging the fluid's and particles' equations of motion without application of small-particle or other approximations. Since there is no existing closure consistent with all three thought experiments, we rigorously derive, without any approximation, a new consistent closure and analyze its mathematical properties (§4). The derivation leaves no freedom of choice, meaning the resulting closure is unique. One of its mathematical properties is the attenuation of generalized-buoyancy force density contributions at short wavelengths. We show that this property prevents Hadamard instabilities even for very simplistic two-fluid models (§5). Finally, in §6, we carry out tests of our and existing closures against coarse-grained data from particle-resolved simulations of sediment transport, a disperse two-phase flow that allows direct access to buoyancy. These tests support our closure.

## 2. Contributions of pseudo-stresses to generalized-buoyancy force

### 2.1. Thought experiment to determine contribution of Reynolds stress

We consider a single neutrally buoyant ( $\rho_s = \rho_f$ ) sphere in a statistically steady, uniform turbulent flow of incompressible Newtonian fluid. The particle's radius  $R$  shall be infinitesimally small ( $R \rightarrow 0$ ), implying  $\beta_s \rightarrow 0$  and that the particle Reynolds numbers based on the fluid-particle velocity difference and based on the fluid velocity gradient vanish. In addition,  $R \rightarrow 0$  means that the system boundaries are, in a relative sense, infinitely far away from the particle. This permits applying the analysis by Maxey & Riley (1983) based on the Stokes equations for the disturbance flow to calculate the time-dependent hydrodynamic force  $\tilde{\mathbf{F}}_h$  acting on the particle. Due to  $R \rightarrow 0$ , only contributions in leading order of  $R$  matter. By imposing that initially ( $t = 0$ ) the particle's center-of-mass velocity  $\mathbf{v}_\uparrow$  and acceleration  $\dot{\mathbf{v}}_\uparrow$  are equal to the background flow velocity  $\tilde{\mathbf{u}}$  and acceleration  $\tilde{D}_t \tilde{\mathbf{u}}$ , respectively, evaluated at its center of mass  $\mathbf{x}_o$ , which ensures that the drag and virtual-mass forces vanish identically, the leading-order contributions are the time-dependent generalized-buoyancy force  $\tilde{\mathbf{F}}_B$ , given by (1.2) or (1.3), and the Faxen force, both of which are  $O(R^3)$ . However, the Faxen force vanishes identically if one replaces the no-slip boundary conditions at the particle's surface by free-slip boundary conditions ( $\beta \rightarrow 0$  in equation (35) of Keh & Chen 1996). Then,  $\tilde{\mathbf{F}}_B$  is the only remaining hydrodynamic force contribution. It means that the particle behaves like a perfect tracer, moving translationally exactly like a fluid parcel of the background flow, i.e.,  $\mathbf{v}_\uparrow[t] = \tilde{\mathbf{u}}[\mathbf{x}_o[t], t]$  for all  $t$ . Hence, using (1.3) and the condition of statistically steady, uniform flow, as well as Reynolds transport theorem,  $\int_{\mathbb{V}} \rho_f \tilde{D}_t \tilde{\mathbf{u}} dV = d_t \int_{\mathbb{V}} \rho_f \tilde{\mathbf{u}} dV$ , we can calculate the average generalized-buoyancy force acting on this tracer particle as

$$\begin{aligned} \mathbf{F}_B &= \lim_{T \rightarrow \infty} \frac{1}{T} \int_0^T \int_{\mathbb{V}} \rho_f (\tilde{D}_t \tilde{\mathbf{u}} - \mathbf{g}) dV dt = \lim_{T \rightarrow \infty} \frac{1}{T} \int_0^T \frac{d}{dt} \int_{\mathbb{V}} \rho_f \tilde{\mathbf{u}} dV dt - \int_{\mathbb{V}} \rho_f \mathbf{g} dV \\ &= - \int_{\mathbb{V}} \rho_f \mathbf{g} dV. \end{aligned} \quad (2.1)$$

At the same time, the ensemble-averaged momentum balance, using  $\beta_s \rightarrow 0$  and the condition of statistically steady, uniform flow, reads (e.g., Pahltz *et al.* 2025)

$$\nabla \cdot (\langle \boldsymbol{\sigma} \rangle + \boldsymbol{\sigma}_{\text{Re}}^f) = -\rho_f \mathbf{g}, \quad (2.2)$$

where  $\boldsymbol{\sigma}$  is the instantaneous, local fluid stress tensor of the actual (background plus disturbance) flow and  $\langle \cdot \rangle$  denotes the ensemble average. Put together, (2.1) and (2.2) imply

$$\mathbf{F}_B = \int_{\mathbb{V}} \nabla \cdot (\langle \boldsymbol{\sigma} \rangle + \boldsymbol{\sigma}_{\text{Re}}^f) dV. \quad (2.3)$$

It means that, for the scenario considered in this thought experiment, the Reynolds stress  $\boldsymbol{\sigma}_{\text{Re}}^f$  fully contributes to the background flow responsible for the average generalized-buoyancy force  $\mathbf{F}_B$ . This result is in agreement with the perhaps only existing empirical evidence on that matter, the experiments by Lamb *et al.* (2017) mentioned in the introduction. Hence, expressions for  $\mathbf{F}_B$  or the generalized-buoyancy force density  $\beta_s \langle \mathbf{f}_B \rangle^s$  that do not involve  $\boldsymbol{\sigma}_{\text{Re}}^f$  (e.g., Zhang *et al.* 2007; Chauchat 2018; Maurin *et al.* 2018) are inconsistent generalizations of buoyancy.

### 2.2. Thought experiment to determine contribution of pseudo-stress due to fluid-particle interactions

We consider a statistically steady, uniform particulate Stokes flow consisting of rigid particles. The dispersed-phase volume fraction  $\beta_s$  is nonzero but sufficiently low to ensure that fluid-

mediated particle-particle interactions are negligible. The particles are identical spheres of a radius  $R$  that is sufficiently smaller than the scale  $L$  over which the macroscopic flow changes. Under these assumptions, in the first order of  $R/L$  and the first order of  $\beta_s$ , the following average fluid phase momentum balance can be derived (equation (55) of Jackson 1997, omitting its term of order  $(R/L)^2$ ):

$$\begin{aligned} \nabla \cdot \left\{ -\langle P \rangle^f \mathbf{1} + \eta_f \left( \nabla \langle \mathbf{u} \rangle + (\nabla \langle \mathbf{u} \rangle)^T \right) + \frac{5\eta_f \beta_s}{2} \left( \nabla \langle \mathbf{u} \rangle^f + (\nabla \langle \mathbf{u} \rangle^f)^T \right) \right. \\ \left. + 3\eta_f \beta_s \left( \frac{1}{2} \left( \nabla \langle \mathbf{u} \rangle^f - (\nabla \langle \mathbf{u} \rangle^f)^T \right) - \epsilon \cdot \langle \boldsymbol{\omega} \rangle^s \right) \right\} \\ - \frac{9\eta_f \beta_s}{2R^2} \left( \langle \mathbf{u} \rangle^f - \langle \mathbf{u}_\uparrow \rangle^s + \frac{R^2}{6} \Delta \langle \mathbf{u} \rangle^f \right) + \rho_f \mathbf{g} = 0, \end{aligned} \quad (2.4)$$

where  $P$  is the instantaneous, local fluid pressure,  $\eta_f$  the clear-fluid viscosity,  $\mathbf{u}$  ( $\mathbf{u}_\uparrow$ ) the instantaneous, local velocity of the fluid or dispersed phase including (excluding) particle-rotational contributions,  $\epsilon$  the total antisymmetric tensor,  $\langle \boldsymbol{\omega} \rangle^s$  the average angular particle velocity, and  $\Delta = \nabla \cdot \nabla$  the Laplace operator. Furthermore,  $\langle \cdot \rangle$ ,  $\langle \cdot \rangle^f$ ,  $\langle \cdot \rangle^s$  denote the mixture, fluid phase, and dispersed-phase averages, respectively (precise definitions are given in §3.1).

The question is now how to interpret the different terms in (2.4). The first term on the third line is readily identified as the negative sum of the drag and Faxen force per unit volume of pure fluid, which are the only terms contributing to generalized drag for steady Stokes flow (Maxey & Riley 1983). However, the actual generalized-drag force density  $\beta_s \langle \mathbf{f}_D \rangle^s$  is the sum of the drag and Faxen force per unit volume of the fluid-particle mixture, since the fluid phase momentum balance, in the context of two-fluid momentum balances, refers to the mixture volume. To translate pure-fluid-based volumetric densities into mixture-based volumetric densities, one has to multiply the former with the fluid volume fraction  $\beta_f$ . Hence, we conclude

$$\beta_s \langle \mathbf{f}_D \rangle^s = \frac{9\eta_f \beta_s \beta_f}{2R^2} \left( \langle \mathbf{u} \rangle^f - \langle \mathbf{u}_\uparrow \rangle^s + \frac{R^2}{6} \Delta \langle \mathbf{u} \rangle^f \right). \quad (2.5)$$

The remaining part  $(\beta_s^2/\beta_f) \langle \mathbf{f}_D \rangle^s$  is therefore attributed to the generalized-buoyancy force density  $\beta_s \langle \mathbf{f}_B \rangle^s$  alongside the usual gravitational term:

$$\beta_s \langle \mathbf{f}_B \rangle^s = \beta_s \left( \beta_f^{-1} \beta_s \langle \mathbf{f}_D \rangle^s - \rho_f \mathbf{g} \right). \quad (2.6)$$

This somewhat odd appearance of drag terms in  $\beta_s \langle \mathbf{f}_B \rangle^s$  was exactly what led to the debate between Clift *et al.* (1987) and others that we briefly discussed in §1. Note that it is not inconsistent with the approximations behind (2.4) to decompose the total fluid-particle interaction force density, which is on the order of  $\beta_s^1$ , into two contribution on the order of  $\beta_s^2$ , (2.5) and (2.6). The only aspect that is required for consistency, including self-consistency of (2.4), is that the leading order of the combination of all the terms on the left-hand side of (2.4) is  $\beta_s^1$ .

The remaining terms in (2.4) are the gravitational body force density  $\beta_f \rho_f \mathbf{g}$  and a divergence of two distinct stress tensors: the fluid-phase-averaged stress tensor (Jackson 1997),

$$\beta_f \langle \boldsymbol{\sigma} \rangle^f = -\beta_f \langle P \rangle^f \mathbf{1} + \eta_f \left( \nabla \langle \mathbf{u} \rangle + (\nabla \langle \mathbf{u} \rangle)^T \right), \quad (2.7)$$

and a pseudo-stress tensor  $\boldsymbol{\sigma}_s^f$  that has emerged due to fluid-particle interactions (Jackson

1997),

$$\sigma_s^f = -\beta_s \langle P \rangle^f \mathbf{1} + \frac{5\eta_f \beta_s}{2} \left( \nabla \langle \mathbf{u} \rangle^f + \left( \nabla \langle \mathbf{u} \rangle^f \right)^T \right) + 3\eta_f \beta_s \left( \frac{1}{2} \left( \nabla \langle \mathbf{u} \rangle^f - \left( \nabla \langle \mathbf{u} \rangle^f \right)^T \right) - \boldsymbol{\epsilon} \cdot \langle \boldsymbol{\omega} \rangle^s \right). \quad (2.8)$$

Using (2.5)-(2.8), we can rewrite (2.4) in either of the following two forms:

$$\nabla \cdot \left( \beta_f \langle \boldsymbol{\sigma} \rangle^f + \boldsymbol{\sigma}_s^f \right) + \beta_f \rho_f \mathbf{g} - \beta_s \langle \mathbf{f}_D \rangle^s - \beta_s \langle \mathbf{f}_B \rangle^s = 0, \quad (2.9)$$

$$\nabla \cdot \left( \beta_f \langle \boldsymbol{\sigma} \rangle^f + \boldsymbol{\sigma}_s^f \right) + \rho_f \mathbf{g} - \beta_f^{-1} \beta_s \langle \mathbf{f}_D \rangle^s = 0. \quad (2.10)$$

Multiplying (2.10) with  $\beta_f$  and subtracting the result from (2.9) then yields

$$\beta_s \langle \mathbf{f}_B \rangle^s = \beta_s \nabla \cdot \left( \beta_f \langle \boldsymbol{\sigma} \rangle^f + \boldsymbol{\sigma}_s^f \right). \quad (2.11)$$

It means that, for the scenario considered in this thought experiment, the pseudo-stress  $\boldsymbol{\sigma}_s^f$  fully contributes to the background flow responsible for the generalized-buoyancy force density  $\beta_s \langle \mathbf{f}_B \rangle^s$ . Hence, expressions for  $\beta_s \langle \mathbf{f}_B \rangle^s$  that do not fully incorporate  $\boldsymbol{\sigma}_s^f$ —for example, Zhang *et al.* (2007) and Maurin *et al.* (2018) only account for the portion of  $\boldsymbol{\sigma}_s^f$  that is equal to  $\beta_s \langle \boldsymbol{\sigma} \rangle^f$ —are inconsistent generalizations of buoyancy.

### 2.3. Conclusion from thought experiments supported by physical intuition

Noting that  $\langle \boldsymbol{\sigma} \rangle = \beta_f \langle \boldsymbol{\sigma} \rangle^f$  for the thought experiment in §2.1 due to  $\beta_f = 1$ , and that both thought experiments require the particle(s) to be small, we come to the conclusion that, for sufficiently small particles,

$$\boldsymbol{\sigma}^f \equiv \beta_f \langle \boldsymbol{\sigma} \rangle^f + \boldsymbol{\sigma}_{\text{Re}}^f + \boldsymbol{\sigma}_s^f \quad (2.12)$$

is the background flow stress responsible for buoyancy in general disperse two-phase flow. In fact, (2.12) is the only expression based on the fluid-phase-averaged stress  $\beta_f \langle \boldsymbol{\sigma} \rangle^f$  and the two pseudo-stresses  $\boldsymbol{\sigma}_{\text{Re}}^f$  and  $\boldsymbol{\sigma}_s^f$ —the only three stresses that can conceivably play a role in the problem—that yields simultaneously  $\beta_f \langle \boldsymbol{\sigma} \rangle^f + \boldsymbol{\sigma}_{\text{Re}}^f$  for  $\boldsymbol{\sigma}_s^f = 0$  and  $\beta_f \langle \boldsymbol{\sigma} \rangle^f + \boldsymbol{\sigma}_s^f$  for  $\boldsymbol{\sigma}_{\text{Re}}^f = 0$ . Hence, the buoyancy closure by Anderson & Jackson (1967),

$$\beta_s \langle \mathbf{f}_B \rangle^s = \beta_s \nabla \cdot \boldsymbol{\sigma}^f, \quad (2.13)$$

is the unique closure consistent with the thought experiments for sufficiently small particles. This finding conforms with physical intuition, since  $\boldsymbol{\sigma}^f$  constitutes the total effective stress in the average fluid phase momentum balance. In fact, in any continuum-like momentum balance equation, the divergence of the total effective stress,  $\nabla \cdot \boldsymbol{\sigma}^f$ , encodes the effect of inner forces applied by the medium on itself. However, in the present situation, the medium is no longer the pure fluid but the fluid portion of a mixture, no longer resolving the smaller scales associated with the pure-fluid flow. Furthermore, the fact that all pseudo-stresses fully contribute to the force applied by the averaged fluid flow is by no means surprising and, in fact, so natural that Jackson (2000), who argued in favor of (2.13), did not even discuss this in their essay about buoyancy. The reason is simply that even the Newtonian stress of the non-averaged Navier-Stokes equations, which is uncontroversially responsible for the total hydrodynamic force acting on a submerged particle, is a stress that originates from pseudo-stresses resulting from averaging processes at (much) smaller scales. For example, in the kinetic theory of gases, which derives the Navier-Stokes equations from the molecular motion, the stresses that eventually lead to the Newtonian stress are Reynolds-like pseudo-stresses encoding the molecular fluctuation motion (Ferziger & Kaper 1972).

### 3. Effect of the small-particle approximation

In §3.2, we present another thought experiment designed to test the compatibility of (2.13) and other existing buoyancy closures with disperse two-phase flows consisting of particles of arbitrary sizes (and shapes and compositions). However, this requires to first introduce (notation-heavy) micromechanical expressions for the terms in the two-fluid momentum balances that are mathematically exact regardless of such particle properties (§3.1).

#### 3.1. Mathematically exact two-fluid momentum balances from averaging the equations of motion

Here, we summarize the results by Pahzt *et al.* (2025) of the derivation of the macroscopic two-fluid momentum balances from averaging the microscopic equations of motion of the fluid and nearly rigid particles. However, note that their assumption of nearly rigid particles (clarified shortly) is not required for the buoyancy-related analysis we perform afterward, in §3.2 and §4.1, since considering deformable and/or compressible particles, such as droplets and bubbles, has no effect on the average fluid phase momentum balance and the micromechanical expressions for the quantities therein as long as interfacial mass transfer does not occur (Fintzi & Pierson 2025). (The case of interfacial mass transfer is addressed at the end of this subsection.)

Pahzt *et al.* (2025) defined the microscopic system as follows: The fluid-particle mixture is contained within the domain  $\mathbb{V}_\infty = \mathbb{V}_f[t] \cup \mathbb{V}_s[t]$  composed of the fluid phase  $\mathbb{V}_f$  and dispersed phase  $\mathbb{V}_s$ . The latter is subdivided into individual particles  $p$ :  $\mathbb{V}_s[t] = \cup_p \mathbb{V}^p[t]$ . The corresponding indicator functions  $X_\infty[\mathbf{x}]$ ,  $X_f[\mathbf{x}, t]$ ,  $X_s[\mathbf{x}, t]$ , and  $X^p[\mathbf{x}, t]$ , with  $\mathbf{x} \in \mathbb{R}^3$  the spatial coordinate, are defined as being equal to 1 within the interiors and equal to 0 outside of  $\mathbb{V}_\infty$ ,  $\mathbb{V}_f$ ,  $\mathbb{V}_s$ , and  $\mathbb{V}^p$ , respectively. The fluid satisfies general microscopic mass and momentum balance equations:

$$\partial_t \rho + \nabla \cdot \rho \mathbf{u} = 0, \quad (3.1)$$

$$\rho(\partial_t \mathbf{u} + \mathbf{u} \cdot \nabla \mathbf{u}) = \nabla \cdot \boldsymbol{\sigma} + \rho \mathbf{g}. \quad (3.2)$$

In contrast to before,  $\boldsymbol{\sigma}$  is a stress tensor associated with an arbitrary fluid flow rheology and the density  $\rho$  is not necessarily constant and therefore distinguished from the previous  $\rho_f$ . In particular, the microscopic fields  $\rho[\mathbf{x}, t]$  and  $\mathbf{u}[\mathbf{x}, t]$  are not only defined for  $\mathbf{x} \in \mathbb{V}_f$  but also for  $\mathbf{x} \in \mathbb{V}^p$ , where they coincide with a particle  $p$ 's (not necessarily constant) interior mass density distribution and its velocity  $\mathbf{v}_\uparrow^p + \boldsymbol{\omega}^p \times \mathbf{r}^p$ , respectively. Here  $\mathbf{v}_\uparrow^p[t]$  is the center-of-mass velocity,  $\boldsymbol{\omega}^p[t]$  the angular velocity, and  $\mathbf{r}^p[\mathbf{x}, t] \equiv \mathbf{x} - \mathbf{x}^p[t]$  the relative coordinate, with  $\mathbf{x}^p[t]$  the center-of-mass location. A density field  $\rho_*$  based on the average mass density  $M^p/V^p$  of each particle  $p$ , with  $M^p$  its mass and  $V^p$  its volume, and a velocity field  $\mathbf{u}_\uparrow$  without particle-rotational contributions are also defined as  $\rho_* \equiv X_f \rho + \sum_p X^p M^p/V^p$  and  $\mathbf{u}_\uparrow \equiv X_f \mathbf{u} + \sum_p X^p \mathbf{v}_\uparrow^p$ , respectively. The particles are non-Brownian and no interfacial mass transfer is allowed to occur (impermeable boundary conditions), implying that the normal velocity  $\mathbf{u} \cdot \mathbf{n}^p$  is continuous at the surface  $\mathbb{S}^p = \partial \mathbb{V}^p$ , where  $\mathbf{n}^p$  is the corresponding unit normal vector pointing outward the particle  $p$ . They experience the instantaneous, local hydrodynamic force  $\mathbf{F}_h^p = \int_{\mathbb{S}^p} \mathbf{n}^p \cdot \boldsymbol{\sigma} dS$ , which defines the microscopic hydrodynamic force density field  $\mathbf{f}_h \equiv \sum_p X^p \mathbf{F}_h^p/V^p$ , and interact via contacts, where slight transient elastic deformations are permitted (i.e., particles are not fully rigid). However, it is assumed that these do not alter the particles' overall shapes significantly and that the contact area of a contacting particle pair  $pq$  can be represented by a single contact point  $\mathbf{x}_c^{pq} = \mathbf{x}_c^{qp}$ . The total contact force acting on a particle  $p$  is denoted as  $\mathbf{F}_c^p = \sum_q \mathbf{F}_c^{pq}$ , resulting from interactions  $\mathbf{F}_c^{pq} = -\mathbf{F}_c^{qp}$  with other particles  $q$  (by convention,  $\mathbf{F}_c^{pp} = 0$ ).

The two-fluid momentum balances result rigorously, without any approximation, from averaging the fluid's and particles' equations of motion using an averaging procedure  $\langle \cdot \rangle$  that satisfies the following rules (Pähtz *et al.* 2025):

$$\langle cA_1 + A_2 \rangle = c\langle A_1 \rangle + \langle A_2 \rangle, \quad \langle \nabla A \rangle = \nabla \langle A \rangle, \quad \langle \partial_t A \rangle = \partial_t \langle A \rangle, \quad \langle AX_\infty \rangle = \langle A \rangle, \quad (3.3)$$

where the  $A$ -s are arbitrary fields well-defined for  $\mathbf{x} \in \mathbb{V}_\infty$ . In addition, for physical reasons such as uniqueness, the Reynolds rule,

$$\langle \langle A_1 \rangle A_2 \rangle = \langle A_1 \rangle \langle A_2 \rangle, \quad (3.4)$$

must also be obeyed. The ensemble average, the infinite time average in statistically steady systems, and infinite averages over spatial coordinates in which the system is homogeneous are the standard examples for averaging procedures that identically satisfy all the rules in (3.3) and (3.4). Based on  $\langle \cdot \rangle$ , phase averages and mass-weighted phase averages are also defined:

$$\langle A \rangle^f \equiv \langle X_f A \rangle / \beta_f, \quad \langle A \rangle^s \equiv \langle X_s A \rangle / \beta_s, \quad \langle A \rangle = \beta_f \langle A \rangle^f + \beta_s \langle A \rangle^s, \quad (3.5)$$

$$\langle A \rangle_{\rho_*}^f \equiv \langle \rho_* A \rangle^f / \rho_f, \quad \langle A \rangle_{\rho_*}^s \equiv \langle \rho_* A \rangle^s / \rho_s, \quad \langle A \rangle_{\rho_*} \equiv \rho_m^{-1} \left( \beta_f \rho_f \langle A \rangle^f + \beta_s \rho_s \langle A \rangle^s \right), \quad (3.6)$$

where  $\beta_f \equiv \langle X_f \rangle$  is the fluid volume fraction,  $\beta_s \equiv \langle X_s \rangle$  the dispersed-phase volume fraction,  $\rho_f \equiv \langle \rho \rangle^f = \langle \rho_* \rangle^f$  the average fluid density,  $\rho_s \equiv \langle \rho_* \rangle^s$  the average dispersed-phase density, and  $\rho_m \equiv \beta_f \rho_f + \beta_s \rho_s$  the average mixture density. Note that these definitions are consistent with our prior usage of these quantities. In particular, the non-averaged value of  $\rho_f$  was considered constant and was therefore identical to the averaged value defined here.

With the above definitions of the microscopic system and averaging procedure, the mathematically exact averaged two-fluid momentum balances can be written as (Pähtz *et al.* 2025)

$$\beta_f \rho_f D_t^f \mathbf{u}_f = \nabla \cdot \boldsymbol{\sigma}^f + \beta_f \rho_f \mathbf{g} - \beta_s \langle \mathbf{f}_h \rangle^s, \quad (3.7)$$

$$\beta_s \rho_s D_t^s \mathbf{u}_s = \nabla \cdot \boldsymbol{\sigma}^s + \beta_s \rho_s \mathbf{g} + \beta_s \langle \mathbf{f}_h \rangle^s, \quad (3.8)$$

where  $\mathbf{u}_f \equiv \langle \mathbf{u} \rangle_{\rho_*}^f = \langle \mathbf{u}_\uparrow \rangle_{\rho_*}^f$  is the average fluid phase velocity,  $\mathbf{u}_s \equiv \langle \mathbf{u}_\uparrow \rangle_{\rho_*}^s$  the average dispersed-phase velocity without particle-rotational contributions,  $D_t^f \equiv \partial_t + \mathbf{u}_f \cdot \nabla$  and  $D_t^s \equiv \partial_t + \langle \mathbf{u} \rangle_{\rho_*}^s \cdot \nabla$  are the associated material derivatives, and  $\boldsymbol{\sigma}^f$  and  $\boldsymbol{\sigma}^s$  the effective fluid phase and dispersed-phase stress tensors, respectively. The latter are given by (Pähtz *et al.* 2025, and their Supplementary Material)

$$\boldsymbol{\sigma}^f \equiv \beta_f \langle \boldsymbol{\sigma} \rangle^f + \boldsymbol{\sigma}_{\text{Re}}^f + \boldsymbol{\sigma}_s^f = \langle \boldsymbol{\sigma} \rangle^f + \boldsymbol{\sigma}_{\text{Re}}^f + \boldsymbol{\sigma}_{s'}^f + [\langle \boldsymbol{\sigma} \rangle^f]_s', \quad (3.9)$$

$$\boldsymbol{\sigma}_{\text{Re}}^f \equiv -\beta_f \rho_f \left\langle (\mathbf{u}_\uparrow - \mathbf{u}_f) (\mathbf{u}_\uparrow - \mathbf{u}_f) \right\rangle_{\rho_*}^f, \quad (3.10)$$

$$\boldsymbol{\sigma}_{s'}^f \equiv \left\langle \sum_p S^p \left( \mathbf{r}^p \mathbf{n}^p \cdot \left( \boldsymbol{\sigma} - \langle \boldsymbol{\sigma} \rangle^f \right) \delta_{\text{Lx}}^p - \mathbf{r}^p \delta_{\text{Lx}}^p \mathbf{n}^p \cdot \left( \boldsymbol{\sigma} - \langle \boldsymbol{\sigma} \rangle^f \right) \right) \right\rangle_{\mathbb{S}^p}, \quad (3.11)$$

$$\boldsymbol{\sigma}^s \equiv \boldsymbol{\sigma}_c^s + \boldsymbol{\sigma}_{\text{Re}}^s, \quad (3.12)$$

$$\boldsymbol{\sigma}_c^s \equiv \left\langle \frac{1}{2} \sum_{pq} \left( \mathbf{r}_c^{pq} \delta_{\text{cLx}}^{pq} - \mathbf{r}_c^{qp} \delta_{\text{cLx}}^{qp} \right) \mathbf{F}_c^{pq} \right\rangle - \left\langle \sum_p \mathbf{r}^p \delta_{\text{Lx}}^p \mathbf{F}_c^p \right\rangle, \quad (3.13)$$

$$\boldsymbol{\sigma}_{\text{Re}}^s \equiv -\beta_s \rho_s \left\langle \left( \mathbf{u} - \langle \mathbf{u} \rangle_{\rho_*}^s \right) (\mathbf{u}_\uparrow - \mathbf{u}_s) \right\rangle_{\rho_*}^s. \quad (3.14)$$

If all particles are spheres, the particle-rotational terms cancel each other out, formally  $\langle \mathbf{u} \rangle_{\rho_*}^s \rightarrow \mathbf{u}_s$  in the definitions of  $D_t^s$  and  $\boldsymbol{\sigma}_{\text{Re}}^s$ . The above expressions involve the operators  $\dot{\cdot}_{\mathbb{V}^p} \equiv \frac{1}{V^p} \int_{\mathbb{V}^p} \cdot dV$  and  $\dot{\cdot}_{\mathbb{S}^p} \equiv \frac{1}{S^p} \int_{\mathbb{S}^p} \cdot dS$ , with  $V^p$  and  $S^p$  the volume and surface area of a

particle  $p$ , respectively, and the definitions

$$\delta_{\mathbf{Lx}}^p[\mathbf{y}] \equiv \int_0^1 \delta[\mathbf{x} - \mathbf{x}^p - \lambda(\mathbf{y} - \mathbf{x}^p)] d\lambda, \quad (3.15)$$

$$\delta_{\mathbf{cLx}}^{pq} \equiv \delta_{\mathbf{Lx}}^p[\mathbf{x}_c^{pq}], \quad (3.16)$$

with  $\delta$  the multivariate delta distribution. For the volume and surface averages over terms involving  $\delta_{\mathbf{Lx}}^p[\mathbf{y}]$ , such as  $\underline{\mathbf{r}^p \delta_{\mathbf{Lx}_{\mathbb{V}p}}^p}$ ,  $\mathbf{y}$ , not  $\mathbf{x}$ , is the coordinate over which is averaged (i.e., the result of the averaging depends on  $\mathbf{x}$ ). Furthermore,  $\boldsymbol{\sigma}^f$  in (3.9) consists of the contribution  $[\langle \boldsymbol{\sigma} \rangle^f]_s'$ , where  $[\cdot]_s'$  denotes an operator that acts on an arbitrary macroscopic tensor field  $\mathbf{A}$  (i.e.,  $\langle \mathbf{A} \rangle = \mathbf{A}$ ) in the following manner:

$$[\mathbf{A}]_s' \equiv \left\langle \sum_p V^p \underline{\mathbf{r}^p} (\nabla \cdot \mathbf{A} - \nabla \cdot \mathbf{A}_{\mathbb{V}p}) \delta_{\mathbf{Lx}_{\mathbb{V}p}}^p \right\rangle. \quad (3.17)$$

In particular, it satisfies the property

$$\nabla \cdot [\mathbf{A}]_s' = (\mathcal{L} - \mathcal{I})\beta_s \nabla \cdot \mathbf{A}, \quad (3.18)$$

where  $\mathcal{I}$  is the identity operator, and the action of the operator  $\mathcal{L}$  is defined through

$$\mathcal{L}\beta_s \mathbf{A} \equiv \beta_s \left\langle \sum_p X^p \underline{\mathbf{A}_{\mathbb{V}p}} \right\rangle^s. \quad (3.19)$$

The operators  $\mathcal{L} - \mathcal{I}$  and  $[\cdot]_s'$  encode the effects of particle-size-related variations of  $\mathbf{A}$  and  $\nabla \cdot \mathbf{A}$ , respectively, and play important roles in the coming calculations. In fact, in the limit of vanishing particle size for non-spherical particles or in the first order of  $R/L$  for spherical particles,  $\mathcal{L} \rightarrow \mathcal{I}$ , which we henceforth term “the small-particle approximation”.

The averaged two-fluid momentum balances (3.7) and (3.8) contain various terms that require closure. However, for the purpose of our analysis, we do not employ any closure but the buoyancy closure, defined as the expression for  $\beta_s \langle \mathbf{f}_B \rangle^s$  that separates generalized-drag contributions  $\beta_s \langle \mathbf{f}_D \rangle^s$  from the total interfacial force density  $\beta_s \langle \mathbf{f}_h \rangle^s$ :

$$\beta_s \langle \mathbf{f}_h \rangle^s = \beta_s \langle \mathbf{f}_B \rangle^s + \beta_s \langle \mathbf{f}_D \rangle^s. \quad (3.20)$$

The goal is to do this in a manner that is mathematically consistent with the exact micromechanical expressions for the other terms in (3.7).

In the case of interfacial mass transfer, the normal component of  $\mathbf{u}$  experiences a jump across the interface, leading to additional stress-divergence terms and source terms in (3.7) and (3.8), respectively, that are coupled to the interface momentum balance (Fintzi & Pierson 2025). In this case, the additional stress-divergence term in (3.7) can be lumped into  $\nabla \cdot \boldsymbol{\sigma}_s^f$  and subsequently  $\nabla \cdot \boldsymbol{\sigma}_{s'}^f$ , and the additional source term in (3.7) into  $-\beta_s \langle \mathbf{f}_h \rangle^s$  and subsequently  $-\beta_s \langle \mathbf{f}_D \rangle^s$  via (3.20), leaving the analysis in §3.2 and §4.1 unchanged.

### 3.2. Thought experiment to determine effects of particle size on buoyancy closures

We define a Cartesian coordinate system  $\mathbf{x} = (x, y, z)$ , where the coordinates  $x$  and  $y$  span the horizontal domain and  $z$  is in the vertical direction aligned with the direction of gravity. We then consider a statistically horizontally homogeneous particle bed immersed in a fluid at rest. The weight density  $\rho_f \mathbf{g}$  of this fluid shall be vertically stratified,  $\rho_f \mathbf{g} = (\rho_f \mathbf{g})(z)$ . This can, for example, be achieved through fluid density stratification or a short distance to the gravitational source’s center of mass. Since the system is statistically homogeneous in the  $x$ - and  $y$ -directions, we choose a spatial average over the infinite  $(x, y)$ -domain as the averaging procedure  $\langle \cdot \rangle$ , which identically satisfies all the rules in (3.3) and (3.4). (This should be equivalent to choosing ensemble averaging.) Due to  $\nabla \cdot \boldsymbol{\sigma} = -\rho_f \mathbf{g}$ , the microscopic fluid

stress tensor  $\sigma$  depends only on  $z$ , implying  $\langle \sigma \rangle^f = \sigma$  and therefore  $\sigma_{s'}^f = 0$ . Furthermore, in this completely stationary scenario,  $u_f = 0$ ,  $\sigma_{\text{Re}}^f = 0$ , and  $\beta_s \langle f_h \rangle^s = \beta_s \langle f_B \rangle^s$ . Put together, using (3.18) and (3.19), (3.7) simplifies to

$$\beta_s \langle f_B \rangle^s = -\mathcal{L} \beta_s \rho_f g. \quad (3.21)$$

In contrast, inserting (2.13), the buoyancy closure by Anderson & Jackson (1967), in (3.7) yields  $\beta_s \langle f_B \rangle^s = -\beta_s \rho_f g$ , regardless of the precise definition of the terms involved in  $\sigma^f$ . Due to the dependence of  $\rho_f g$  on  $z$ , this expression is clearly distinct from (3.21), and the disagreement between the two is the stronger the larger the variations of  $\rho_f g$  within the particles. Only in the small-particle approximation ( $\mathcal{L} \rightarrow \mathcal{I}$ ), the two expressions are equivalent. Similar statements hold for most other existing closures (e.g., Chauchat 2018; Maurin *et al.* 2018). The only existing closure consistent with (3.21), and thus this thought experiment, is  $\beta_s \langle f_B \rangle^s = \mathcal{L} \beta_s \nabla \cdot \langle \sigma \rangle^f$  (Zhang *et al.* 2007), which is, however, inconsistent with the two thought experiments presented in §2. In summary, there is no existing closure consistent with all three thought experiments.

## 4. Unique consistent buoyancy closure

### 4.1. Derivation of closure

We have learned from the three thought experiments that, in the small-particle approximation, the buoyancy closure by Anderson & Jackson (1967), (2.13), is the unique closure consistent with these thought experiments, and that the total effective stress,  $\sigma^f$ , is the only relevant stress in the average fluid phase momentum balance, whereas its constituting stress and pseudo-stress components  $\beta_f \langle \sigma \rangle^f$ ,  $\sigma_{\text{Re}}^f$ , and  $\sigma_s^f$  should not be looked upon in isolation. Furthermore, the thought experiment in §3.2 has also told us that, for a fluid-particle system at complete rest, (3.21) must be satisfied. Using (3.7) for completely stationary conditions (i.e.,  $u_f = 0$ ,  $\sigma_{\text{Re}}^f = 0$ , and  $\beta_s \langle f_h \rangle^s = \beta_s \langle f_B \rangle^s$ ), (3.21) is equivalent to

$$\beta_s \langle f_B \rangle^s = \mathcal{L} \beta_s \beta_f^{-1} \left( \nabla \cdot \sigma^f - \beta_s \langle f_B \rangle^s \right). \quad (4.1)$$

We now relax our viewpoint from completely stationary to general conditions and observe that, in the small-particle approximation ( $\mathcal{L} \rightarrow \mathcal{I}$ ), (4.1) is equivalent to the unique closure associated with this approximation, (2.13). Hence, (4.1) is the unique closure consistent with all three thought experiments. In summary, under the assumptions that a buoyancy closure consistent with all possible disperse two-phase flow scenarios does exist and that the only relevant stress is  $\sigma^f$ , it must be (4.1).

In order to transform the implicit (4.1) into an explicit expression, we define

$$B \equiv \beta_f^{-1} \left( \nabla \cdot \sigma^f - \beta_s \langle f_B \rangle^s \right) = \rho_f D_t^f u_f - \rho_f g + \beta_f^{-1} \beta_s \langle f_D \rangle^s, \quad (4.2)$$

where we used (3.7) and (3.20). Then, (3.7) can be rewritten as

$$B = \nabla \cdot \sigma^f - B', \quad (4.3)$$

where  $\cdot' \equiv (\mathcal{L} - \mathcal{I}) \beta_s \cdot$  is another operator. Repeated application of this operator, using (3.18), then yields

$$B' = \nabla \cdot [\sigma^f]'_s - B'', \quad (4.4)$$

$$B'' = \nabla \cdot \left[ [\sigma^f]'_s \right]'_s - B''', \quad (4.5)$$

and so forth, and therefore

$$\mathbf{B} = \sum_{k=0}^{\infty} (-1)^k \nabla \cdot [\boldsymbol{\sigma}^{\mathbf{f}}]_s'^k, \quad (4.6)$$

where  $[\cdot]_s'^k$  means  $k$  applications of the operator  $[\cdot]_s'$ . Hence, using  $\beta_s \langle \mathbf{f}_B \rangle^s = \mathcal{L} \beta_s \mathbf{B} = \beta_s \mathbf{B} + \mathbf{B}'$  and (4.2), we obtain the following four explicit expressions equivalent to (4.1):

$$\beta_s \langle \mathbf{f}_B \rangle^s = \mathcal{L} \beta_s \left( \rho_f D_t^f \mathbf{u}_f - \rho_f \mathbf{g} + \beta_f^{-1} \beta_s \langle \mathbf{f}_D \rangle^s \right), \quad (4.7)$$

$$\beta_s \langle \mathbf{f}_B \rangle^s = \nabla \cdot \boldsymbol{\sigma}^{\mathbf{f}} - \beta_f \nabla \cdot \hat{\boldsymbol{\sigma}}^{\mathbf{f}}, \quad (4.8)$$

$$\beta_s \langle \mathbf{f}_B \rangle^s = \beta_s \nabla \cdot \hat{\boldsymbol{\sigma}}^{\mathbf{f}} + \nabla \cdot [\hat{\boldsymbol{\sigma}}^{\mathbf{f}}]_s', \quad (4.9)$$

$$\beta_s \langle \mathbf{f}_B \rangle^s = \mathcal{L} \beta_s \nabla \cdot \hat{\boldsymbol{\sigma}}^{\mathbf{f}}, \quad (4.10)$$

where  $\hat{\boldsymbol{\sigma}}^{\mathbf{f}}$  is a modified effective fluid phase stress tensor defined as

$$\hat{\boldsymbol{\sigma}}^{\mathbf{f}} \equiv \sum_{k=0}^{\infty} (-1)^k [\boldsymbol{\sigma}^{\mathbf{f}}]_s'^k = ([\cdot]_s' + \mathcal{I})^{-1} \boldsymbol{\sigma}^{\mathbf{f}}. \quad (4.11)$$

Using (3.18), the latter also satisfies

$$\nabla \cdot \hat{\boldsymbol{\sigma}}^{\mathbf{f}} = \sum_{k=0}^{\infty} (-1)^k (\mathcal{L} \beta_s \cdot - \mathcal{I} \beta_s \cdot)^k \nabla \cdot \boldsymbol{\sigma}^{\mathbf{f}} = (\mathcal{L} \beta_s \cdot + \mathcal{I} \beta_f \cdot)^{-1} \nabla \cdot \boldsymbol{\sigma}^{\mathbf{f}}. \quad (4.12)$$

From (4.7) and (4.10), using (3.19), we also glean two equivalent expressions for the average generalized-buoyancy force  $\mathbf{F}_B$  acting on a particle occupying the domain  $\mathbb{V}$ :

$$\mathbf{F}_B = \int_{\mathbb{V}} \nabla \cdot \hat{\boldsymbol{\sigma}}^{\mathbf{f}} dV, \quad (4.13)$$

$$\mathbf{F}_B = \int_{\mathbb{V}} \left( \rho_f D_t^f \mathbf{u}_f - \rho_f \mathbf{g} + \beta_f^{-1} \beta_s \langle \mathbf{f}_D \rangle^s \right) dV. \quad (4.14)$$

Equation (4.13) implies that, for general disperse two-phase flow,  $\hat{\boldsymbol{\sigma}}^{\mathbf{f}}$  is the analog to  $\tilde{\boldsymbol{\sigma}}$  in (1.2), while (4.14) is the counterpart to (1.3). Note that the latter considers only a single particle in an infinite flow domain and therefore essentially assumes  $\beta_s \rightarrow 0$ , in which case both expressions are equivalent but for the averaging involved in (4.14).

#### 4.2. Resulting two-fluid momentum balances

There are four distinct meaningful ways to express the two-fluid momentum balances resulting from the unique consistent buoyancy closure. First, inserting (4.7) into (3.7) and (3.8), using (3.20), yields

$$\beta_f \rho_f D_t^f \mathbf{u}_f = \nabla \cdot \boldsymbol{\sigma}^{\mathbf{f}} + \beta_f \rho_f \mathbf{g} - \mathcal{L} \beta_s \left( \rho_f D_t^f \mathbf{u}_f - \rho_f \mathbf{g} + \beta_f^{-1} \beta_s \langle \mathbf{f}_D \rangle^s \right) - \beta_s \langle \mathbf{f}_D \rangle^s, \quad (4.15)$$

$$\beta_s \rho_s D_t^s \mathbf{u}_s = \nabla \cdot \boldsymbol{\sigma}^{\mathbf{s}} + \beta_s \rho_s \mathbf{g} + \mathcal{L} \beta_s \left( \rho_f D_t^f \mathbf{u}_f - \rho_f \mathbf{g} + \beta_f^{-1} \beta_s \langle \mathbf{f}_D \rangle^s \right) + \beta_s \langle \mathbf{f}_D \rangle^s. \quad (4.16)$$

Second, substituting (4.8) into (3.7) and (4.10) into (3.8), using (3.20), results in

$$\beta_f \rho_f D_t^f \mathbf{u}_f = \beta_f \nabla \cdot \hat{\boldsymbol{\sigma}}^{\mathbf{f}} + \beta_f \rho_f \mathbf{g} - \beta_s \langle \mathbf{f}_D \rangle^s, \quad (4.17)$$

$$\beta_s \rho_s D_t^s \mathbf{u}_s = \mathcal{L} \beta_s \nabla \cdot \hat{\boldsymbol{\sigma}}^{\mathbf{f}} + \nabla \cdot \boldsymbol{\sigma}^{\mathbf{s}} + \beta_s \rho_s \mathbf{g} + \beta_s \langle \mathbf{f}_D \rangle^s. \quad (4.18)$$

Third, inserting (4.8) in (3.7) and (4.9) in (3.8), using (3.20), yields

$$\beta_f \rho_f D_t^f \mathbf{u}_f = \beta_f \nabla \cdot \hat{\boldsymbol{\sigma}}^f + \beta_f \rho_f \mathbf{g} - \beta_s \langle \mathbf{f}_D \rangle^s, \quad (4.19)$$

$$\beta_s \rho_s D_t^s \mathbf{u}_s = \beta_s \nabla \cdot \hat{\boldsymbol{\sigma}}^f + \nabla \cdot \hat{\boldsymbol{\sigma}}^s + \beta_s \rho_s \mathbf{g} + \beta_s \langle \mathbf{f}_D \rangle^s, \quad (4.20)$$

where  $\hat{\boldsymbol{\sigma}}^s \equiv \boldsymbol{\sigma}^s + [\hat{\boldsymbol{\sigma}}^f]_s'$  is a modified effective dispersed-phase stress tensor. Fourth, (4.19) and (4.20) can be rearranged and brought into the respective forms

$$\beta_f \rho_f D_t^f \mathbf{u}_f = \nabla \cdot \hat{\boldsymbol{\sigma}}^f + \beta_f \rho_f \mathbf{g} - \beta_s \left( \rho_f D_t^f \mathbf{u}_f - \rho_f \mathbf{g} \right) - \beta_f^{-1} \beta_s \langle \mathbf{f}_D \rangle^s, \quad (4.21)$$

$$\beta_s \rho_s D_t^s \mathbf{u}_s = \nabla \cdot \hat{\boldsymbol{\sigma}}^s + \beta_s \rho_s \mathbf{g} + \beta_s \left( \rho_f D_t^f \mathbf{u}_f - \rho_f \mathbf{g} \right) + \beta_f^{-1} \beta_s \langle \mathbf{f}_D \rangle^s. \quad (4.22)$$

Equations (4.19) and (4.20), as well as (4.21) and (4.22), exhibit the same topological form as the two-fluid momentum balances in Jackson (2000) after inserting their buoyancy closure, though notice the physically important difference that a stress of fluid phase origin,  $[\hat{\boldsymbol{\sigma}}^f]_s'$ , contributes to the effective dispersed-phase stress  $\hat{\boldsymbol{\sigma}}^s$ . In contrast, (4.15) and (4.16), as well as (4.17) and (4.18), are topologically distinct from their counterparts in Jackson (2000) due to their involvement of the operator  $\mathcal{L}$ .

#### 4.3. Effect of $\mathcal{L}$ for a mixture of continuous fluid and identically-sized spheres

The mathematical effect of the operator  $\mathcal{L}$  in (4.15), (4.16), and (4.18) can be fully understood for the simplified case of a disperse two-phase flow in which all particles are spheres of the same radius  $R$  and volume  $V = 4\pi R^3/3$ . In this case, a straightforward calculation (Appendix A) shows that the action of  $\mathcal{L}$  can be expressed in real and Fourier space, respectively, as

$$\mathcal{L}\beta_s \mathbf{A} = \mathcal{M} \left( \mathcal{M}^{-1} \beta_s \right) \mathcal{M} \mathbf{A}, \quad (4.23)$$

$$\mathcal{F} \mathcal{L}\beta_s \mathbf{A} = M_{\hat{k}} \left( M_{\hat{k}}^{-1} \mathcal{F} \beta_s * M_{\hat{k}} \mathcal{F} \mathbf{A} \right), \quad (4.24)$$

where  $\mathcal{F}$  denotes the Fourier transformation,  $*$  the convolution,  $\mathcal{M}$  is the averaging operator defined by (A 4) or through  $\mathcal{M} \mathbf{A}[\mathbf{x}] = \frac{1}{V} \int_{|\mathbf{r}| < R} \mathbf{A}[\mathbf{x} - \mathbf{r}] dV_r$ , and  $M_{\hat{k}}$  its Fourier transform given by

$$M_{\hat{k}} = \sum_{j=0}^{\infty} \frac{3(i\hat{k})^{2j}}{(2j+1)!(2j+3)} = \frac{3(\sin \hat{k} - \hat{k} \cos \hat{k})}{\hat{k}^3}, \quad (4.25)$$

with  $\hat{k} \equiv R|\mathbf{k}|$  the nondimensionalized absolute value of the wavenumber vector  $\mathbf{k}$  spanning the Fourier space. The effect of  $\mathcal{L}$  becomes clear once (4.24) is compared with

$$\mathcal{F}\beta_s \mathbf{A} = \mathcal{F}\beta_s * \mathcal{F} \mathbf{A}. \quad (4.26)$$

It can be seen that  $\mathcal{L}$  modulates the field  $\beta_s \mathbf{A}$  in Fourier space via the function  $M_{\hat{k}}$ , which is essentially a low-pass filter that cuts off large- $\hat{k}$  contributions, while approaching unity in the limit  $\hat{k} \rightarrow 0$  (figure 1). Note that  $\mathcal{M}^{-1} \beta_s = nV$ , where  $n$  is the number density, and, thus,  $M_{\hat{k}}^{-1} \mathcal{F} \beta_s = V \mathcal{F} n$ , implying  $M_{\hat{k}}^{-1} \mathcal{F} \beta_s$  in (4.24) is well-defined for values of  $\mathbf{k}$  where  $M_{\hat{k}} = 0$  due to  $\mathcal{F}\beta_s[\mathbf{k}] = 0$ .

Choosing  $\mathbf{A} = \rho_f D_t^f \mathbf{u}_f - \rho_f \mathbf{g} + \beta_f^{-1} \beta_s \langle \mathbf{f}_D \rangle^s$  in (4.26) results in the Fourier transform of the buoyancy closure by Anderson & Jackson (1967), whereas the same choice in (4.24) yields the Fourier transform of the unique consistent closure derived in this study, (4.7). Hence, at least for identical spherical particles, the latter is essentially a low-pass-filtered version of the former closure.

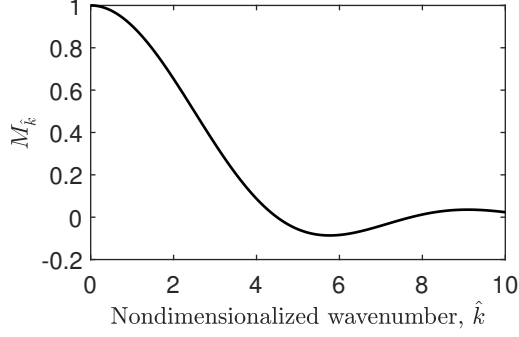


Figure 1: The Fourier transform  $M_{\hat{k}}$  of the averaging operator  $\mathcal{M}$  essentially acts like a low-pass filter, cutting off contributions from wavenumber vectors  $\mathbf{k}$  with  $\hat{k} \equiv R|\mathbf{k}| \gtrsim 4$ .

## 5. Implications for two-fluid models

### 5.1. Well-posedness of two-fluid models

To analyze whether two-fluid models are well-posed when employing our buoyancy closure, we use the form of the momentum balances in (4.17) and (4.18), combined with (4.12), and consider first the simplest possible two-fluid model, the dissipation-free one-pressure model (Stewart & Wendroff 1984), resulting from the closure relations  $\sigma^f = -P_f \mathbf{I}$ ,  $\sigma^s = 0$ , and  $\beta_s \langle \mathbf{f}_D \rangle^s = 0$ :

$$\partial_t \beta_f \rho_f + \nabla \cdot \beta_f \rho_f \mathbf{u}_f = 0, \quad (5.1)$$

$$\partial_t \beta_s \rho_s + \nabla \cdot \beta_s \rho_s \mathbf{u}_s = 0, \quad (5.2)$$

$$\beta_f \rho_f D_t^f \mathbf{u}_f + \beta_f (\mathcal{L} \beta_s \cdot + \mathcal{I} \beta_f \cdot)^{-1} \nabla P_f = \beta_f \rho_f \mathbf{g}, \quad (5.3)$$

$$\beta_s \rho_s D_t^s \mathbf{u}_s + \mathcal{L} \beta_s (\mathcal{L} \beta_s \cdot + \mathcal{I} \beta_f \cdot)^{-1} \nabla P_f = \beta_s \rho_s \mathbf{g}, \quad (5.4)$$

where  $P_f$  is the effective fluid phase pressure and (5.1) and (5.2) are the fluid and dispersed-phase mass balances (Pähtz *et al.* 2025). The model is closed by the volume fraction condition  $\beta_f + \beta_s = 1$  and two equations of state,  $\rho_s = \text{const}$  and  $\rho_f = \rho_f[P_f]$ , with  $\rho'_f \geq 0$ . If this simple model is well-posed, so will be most of the more complex two-fluid models used in the chemical engineering community (see Lhuillier *et al.* 2013, for an overview) as they usually incorporate more dissipative mechanisms. (Non-dissipative virtual-mass forces are addressed at the end of this subsection).

To test for well-posedness, we define  $\mathbf{X} \equiv (\beta_s, u_s, u_f, P_f)^T$ , with  $u_f \equiv u_{fx}$  and  $u_s \equiv u_{sx}$ , and consider small one-spatial-dimensional perturbations  $\mathbf{X}_*(x, t)$  of  $\mathbf{X}$  around a base state  $\mathbf{X}_0$ :

$$\mathbf{X} = \mathbf{X}_0 + \mathbf{X}_*. \quad (5.5)$$

Linearizing (5.1)-(5.4) in  $\mathbf{X}_*$  then yields

$$\mathbf{A}_0 \partial_t \mathbf{X}_* + \mathbf{B}_0 \partial_x \mathbf{X}_* = \mathbf{C}_0, \quad (5.6)$$

where  $\mathbf{A}$ ,  $\mathbf{B}$ , and  $\mathbf{C}$  are given by

$$\mathbf{A} \equiv \begin{pmatrix} -\rho_f & 0 & 0 & (1 - \beta_s)\rho'_f \\ \rho_s & 0 & 0 & 0 \\ 0 & 0 & \rho_f & 0 \\ 0 & \rho_s & 0 & 0 \end{pmatrix}, \quad \mathbf{C} \equiv \begin{pmatrix} 0 \\ 0 \\ \rho_f \mathbf{g} \\ \rho_s \mathbf{g} \end{pmatrix}, \quad (5.7)$$

$$\mathbf{B} \equiv \begin{pmatrix} -\rho_f u_f & 0 & (1 - \beta_s)\rho_f & (1 - \beta_s)u_f \rho'_f \\ \rho_s u_s & \beta_s \rho_s & 0 & 0 \\ 0 & 0 & \rho_f u_f & (\beta_s \mathcal{M}^2 + (1 - \beta_s)\mathcal{I})^{-1} \\ 0 & \rho_s u_s & 0 & \mathcal{M}^2 (\beta_s \mathcal{M}^2 + (1 - \beta_s)\mathcal{I})^{-1} \end{pmatrix}.$$

Note that we used (4.23), assuming identically-sized spheres for simplicity (discussed shortly). Now, we Fourier-transform (5.6), formally  $\partial_x \rightarrow ik$  and  $\mathcal{M} \rightarrow M_{\hat{k}}$ , and keep only the terms dominant in  $k \equiv k_x$ , since we are interested in the limit  $k \rightarrow \infty$  relevant for a Hadamard instability. Formally, this implies

$$\mathbf{C} \rightarrow 0, \quad (\beta_s \mathcal{M}^2 + (1 - \beta_s)\mathcal{I})^{-1} \rightarrow \frac{1}{1 - \beta_s}, \quad \mathcal{M}^2 (\beta_s \mathcal{M}^2 + (1 - \beta_s)\mathcal{I})^{-1} \rightarrow 0 \quad (5.8)$$

in (5.7), since  $M_{\hat{k}}^2 \sim k^{-4}$ . Looking for wave solutions of the form  $\sim \exp(-i\lambda t)$  in the resulting equation, formally  $\partial_t \rightarrow -i\lambda$ , yields a linear system of equations that can be solved for the frequency  $\lambda$ . It exhibits four solutions, two of which coincide:

$$\lambda_{1,2} = u_s k, \quad \lambda_{3,4} = \left( u_f \pm (\beta_f \rho'_f)^{-1/2} \right)_0 k. \quad (5.9)$$

If  $\rho'_f = 0$ , there are only the two solutions  $\lambda_1$  and  $\lambda_2$ . Due to the constraint  $\rho'_f \geq 0$ , all solutions are real, meaning that the dissipation-free one-pressure model is weakly hyperbolic. However, it is not strictly hyperbolic or well-posed, since the eigenvalues  $\lambda_1/k$  and  $\lambda_2/k$  and their corresponding eigenvectors coincide, implying that perturbations grow as  $\sim k^{1/2}$  (Langham *et al.* 2025). In contrast, they grow as  $\sim k^1$  when using previous buoyancy closures based on the small-particle approximation (Stewart & Wendroff 1984), formally obtained by replacing  $\mathcal{M} \rightarrow \mathcal{I}$  in (5.7).

Since, when employing our buoyancy closure, even the simplest two-fluid model is on the verge of being hyperbolic, one only needs to introduce the slightest bit of physics to make it well-posed. For example, any effective dispersed-phase pressure  $P_s[\beta_s]$ , i.e.,  $\sigma^s = -P_s \mathbf{I}$ , with the physically natural property  $P'_s > 0$  resolves the issue. It modifies (5.4) to

$$\beta_s \rho_s \mathbf{D}_t^s \mathbf{u}_s + P'_s \nabla \beta_s + \mathcal{L} \beta_s (\mathcal{L} \beta_s \cdot + \mathcal{I} \beta_f \cdot)^{-1} \nabla P_f = \beta_s \rho_s \mathbf{g}, \quad (5.10)$$

and, as a consequence, the frequencies  $\lambda_1$  and  $\lambda_2$  to

$$\lambda_{1,2} = \left( u_s \pm \sqrt{P'_s / \rho_s} \right)_0 k, \quad (5.11)$$

whilst having no effect on the existence or values of  $\lambda_3$  and  $\lambda_4$ . Since  $\lambda_1$  and  $\lambda_2$  are now distinct, the system of PDEs is well-posed if either the fluid is incompressible,  $\rho'_f = 0$ , or the fluid is compressible,  $\rho'_f > 0$ , and the eigenvalues  $\lambda_1/k$  and  $\lambda_2/k$  do not coincide with  $\lambda_3/k$  and  $\lambda_4/k$ :

$$u_s \pm \sqrt{P'_s / \rho_s} \neq u_f \pm (\beta_f \rho'_f)^{-1/2} \quad \wedge \quad u_s \pm \sqrt{P'_s / \rho_s} \neq u_f \mp (\beta_f \rho'_f)^{-1/2}. \quad (5.12)$$

In contrast, if any of these four inequalities does not hold, the system is ill-posed, since two of the four corresponding eigenvectors turn out to also coincide in this case. Fortunately, in almost all two-phase flow scenarios, the four inequalities in (5.12) are satisfied in the entire

fluid-particle domain, since the speed of sound of the fluid phase,  $(\beta_f \rho_f')^{-1/2}$ , is typically several orders of magnitude larger than any of the other involved quantities:

$$(\beta_f \rho_f')^{-1/2} \gg |u_s|, |u_f|, \sqrt{P_s'/\rho_s}. \quad (5.13)$$

In conclusion, introducing minimal physics into the simplest two-fluid model leads to a well-posed system of PDEs when employing our buoyancy closure, except in very extraordinary circumstances.

In the above analysis, we have argued on the basis of (4.23), which is valid only for systems of identically-sized spheres. However, it is straightforward to generalize this analysis to arbitrary particle sizes and shapes, giving the very same result. This is because the very definition of the operator  $\mathcal{L}$  in (3.19) always means that spatial variations smaller than the characteristic particle size are smoothed out, diminishing buoyancy effects when  $k \rightarrow \infty$ . Furthermore, essentially the same kind of smoothing effect occurs also for the virtual-mass force density  $\beta_s \langle f_{\text{VM}} \rangle^s \equiv \beta_s \langle \sum_p X^p \mathbf{F}_{\text{VM}}^p / V^p \rangle^s$ , which has also been linked to the ill-posedness of two-fluid models (Lhuillier *et al.* 2013). In fact, from generalizing the analysis by Maxey & Riley (1983) to arbitrary  $R/L$  (Appendix B), it turns out that the virtual-mass force  $\mathbf{F}_{\text{VM}}^p$  on a spherical particle  $p$ , like the generalized-buoyancy force  $\mathbf{F}_B^p = V^p \mathcal{M} \nabla \cdot \hat{\boldsymbol{\sigma}}^f$  from (4.13), also involves volume integration,  $\mathbf{F}_{\text{VM}}^p = \frac{1}{2} \rho_f V^p (\mathcal{M} \tilde{\mathbf{D}}_t \tilde{\mathbf{u}}[\mathbf{x}^p] - \dot{\mathbf{v}}_\uparrow^p)$ , encoded in the operator  $V^p \mathcal{M}$ . And, analogous to the buoyancy analysis, the latter expression leads to (Appendix B)

$$\beta_s \langle f_{\text{VM}} \rangle^s = \frac{\rho_f}{2} (\mathcal{L} \beta_s \mathbf{D}_t^m \mathbf{u}_m - \beta_s \mathbf{D}_t^s \mathbf{u}_s), \quad (5.14)$$

where  $\mathbf{u}_m = \beta_f \mathbf{u}_f + \beta_s \mathbf{u}_s$  is the mixture velocity and  $\mathbf{D}_t^m \equiv \partial_t + \mathbf{u}_m \cdot \nabla$  the associated material derivative. Incorporating this virtual-mass force density into the fluid and dispersed-phase momentum balances, (5.3) and (5.10), does not alter the hyperbolicity characteristics, whereas incorporating the standard form,  $\mathcal{L} \rightarrow \mathcal{I}$  in (5.14) (Jackson 2000), results in ill-posedness.

### 5.2. Numerical implementation in two-fluid models

We suggest to use the form of the two-fluid momentum balances in (4.15) and (4.16) when numerically implementing our buoyancy closure in two-fluid models, since it involves no modification of the effective fluid phase stress  $\boldsymbol{\sigma}^f$ , while the operator  $\mathcal{L}$  is applied on only the single term  $\beta_s \mathbf{A}$ , with  $\mathbf{A} = \rho_f \mathbf{D}_t^f \mathbf{u}_f - \rho_f \mathbf{g} + \beta_f^{-1} \beta_s \langle f_D \rangle^s$ . Then, despite the mathematical complexity involved in  $\mathcal{L}$ , there is a simple approximate manner with which its effects can be accounted for:

$$\mathcal{L} \beta_s \mathbf{A} \approx \beta_s \mathcal{M}^2 \mathbf{A}, \quad (5.15)$$

where the radius  $R$  involved in the definition of  $\mathcal{M}$  should, in the case of arbitrarily sized and shaped particles, be interpreted as the volume-equivalent radius corresponding to the average particle volume. Equation (5.15) preserves the regularization effect of  $\mathcal{L}$  and, in the case of identically-sized spheres, agrees with the exact expression for both extreme limits in which either of the two quantities  $\beta_s$  and  $\mathbf{A}$  spatially varies much more than the other one. The numerical implementation of  $\mathcal{M}^2 \mathbf{A}$  is simple. Presume  $\mathbf{A}$  is given for every numerical grid cell  $\mathbf{x}_i$ . Then, assign to each grid cell the value of  $\mathbf{A}$  averaged over a ball of radius  $R$  centered at  $\mathbf{x}_i$ , giving  $\mathcal{M} \mathbf{A}[\mathbf{x}_i]$ . Repeating the procedure for  $\mathcal{M} \mathbf{A}[\mathbf{x}_i]$  results in  $\mathcal{M}^2 \mathbf{A}[\mathbf{x}_i]$ .

## 6. Testing buoyancy closures with DNS-DEM simulations of sediment transport

To test our and existing buoyancy closures, a Direct Numerical Simulation (DNS), based on the Immersed Boundary Method (IBM), is coupled with a Discrete Element Method (DEM)

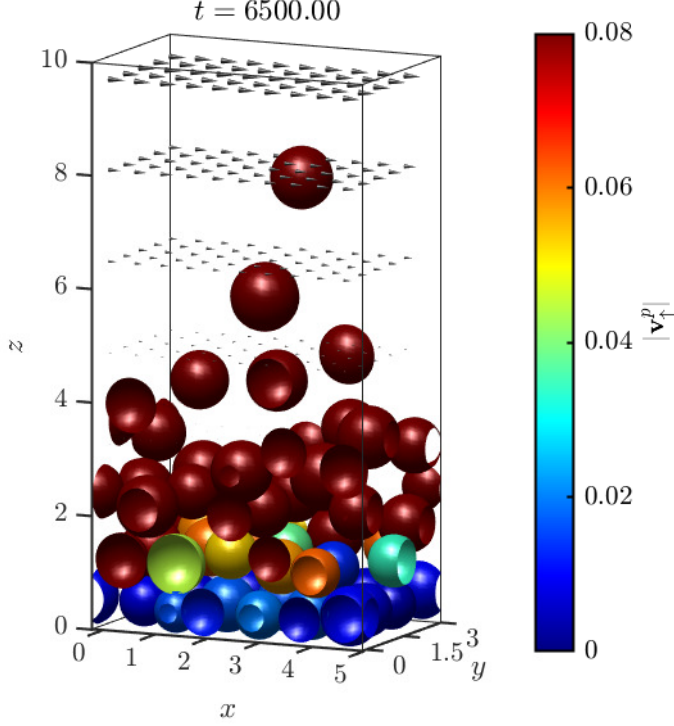


Figure 2: Snapshot of a DNS-DEM simulation of statistically steady, uniform sediment transport for viscosity  $\eta_f = 0.05$ .

to simulate statistically steady, uniform sediment transport (figure 2). This system is one of the few disperse two-phase flows where  $R$  is on the order of  $L$  or even larger due to a typically sudden transition from a densely packed bed to a potentially very dilute transport layer (Chassagne *et al.* 2023; Tholen *et al.* 2023; Fry *et al.* 2024). It is also characterized by a typically negligible generalized-drag force density in the bed-normal direction (explained shortly), a property that allows direct access to buoyancy.

The numerical model is described in detail by Biegert *et al.* (2017) and Zhu *et al.* (2022), based on the IBM after Uhlmann (2005). The gravitational acceleration  $\mathbf{g}$  is driving both the liquid flow and granular particles down a small slope of  $3^\circ$ . Physical quantities are measured in natural units of  $\rho_f$ ,  $(\rho_s/\rho_f - 1)|\mathbf{g}|$ , and  $2R$ . Simulations are conducted for  $\rho_s = 2.65$  and four different viscosities  $\eta_f = [0.1, 0.05, 0.01, 0.001]$ . The flow direction is  $x$ , the direction normal to the bed is  $z$ , and the lateral direction is  $y$ . The system dimensions are  $(L_x, L_y, H) = (5, 3, 15)$ , and 50 identical, spherical particles are considered, forming a bed of approximately three particle layers, with the top layer being the most mobile (figure 2).

The fluid's and particles' equation of motion are averaged using the following averaging procedure:

$$\langle A \rangle[z_n] \equiv \frac{1}{N_T L_x L_y \Delta z} \sum_{k=1}^{N_T} \int_{z_n - \Delta z/2}^{z_n + \Delta z/2} \int_0^{L_y} \int_0^{L_x} A[\mathbf{x}, t_k] dx dy dz, \quad (6.1)$$

which satisfies the rules in (3.3). Due to statistical bed-tangential homogeneity ( $\partial_x = \partial_y = 0$ ), the averaging takes place over the entire bed-tangential domain,  $x \in [0, L_x)$  and  $y \in [0, L_y)$  (periodic boundary conditions), and, due to statistical steadiness, over a sufficient number

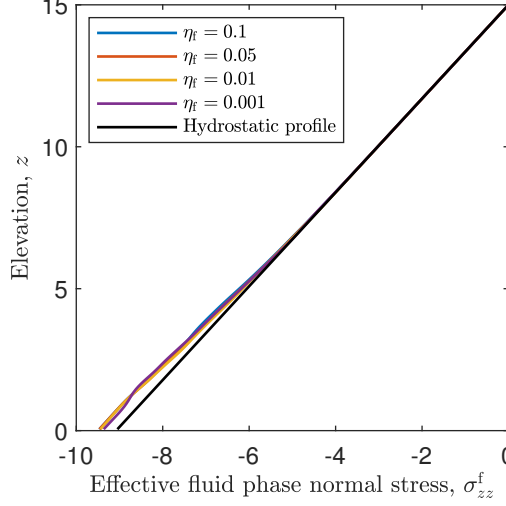


Figure 3: The DNS-DEM simulations of statistically steady, uniform sediment transport exhibit nearly hydrostatic profiles of the effective fluid phase stress  $\sigma_{zz}^f$ .

$N_T = 160$  of timewise *well-separated* instants  $t_k$  to ensure  $\partial_t \approx 0$ . Furthermore,  $\Delta z = 0.1$  is the constant extent of the intervals with centers  $z_n$  that discretize the bed-normal domain  $z \in (0, H)$ . It is twice the DNS grid length and sufficiently small to ensure that (6.1) approximately satisfies the Reynolds rule, (3.4).

Due to  $\partial_x = \partial_y = \partial_t = 0$ , the fluid-phase-averaged vertical momentum balance, (3.7), takes the simple form

$$d_z \sigma_{zz}^f = -\beta_f \rho_f g_z + \beta_s \langle f_{hz} \rangle^s. \quad (6.2)$$

We use (6.2) to calculate  $\sigma_{zz}^f$  indirectly from integrating its right-hand side, which is more accurate than the direct calculation, since the contribution of  $\sigma_{szz}^f$  to  $\sigma_{zz}^f$  in (3.9) is cumbersome to numerically evaluate for the IBM method (Pähtz *et al.* 2025). All other coarse-grained quantities are computed directly as described by Pähtz *et al.* (2025).

The vertical profiles of  $\sigma_{zz}^f$  are approximately hydrostatic (figure 3), implying

$$\beta_s \langle f_{hz} \rangle^s \approx -\beta_s \rho_f g_z \quad (6.3)$$

because of (6.2). Furthermore, it is well-established that, for statistically steady, uniform sediment transport, the vertical generalized-drag force density tends to be negligibly small compared with the submerged particle weight (Bagnold 1956; Chepil 1961; Berzi & Fraccarollo 2013; Li *et al.* 2019; Pähtz & Durán 2018, 2020):

$$\beta_s \langle f_{Dz} \rangle^s \approx 0. \quad (6.4)$$

In fact, there are numerous analytical transport models based on this approximation, and they have been very successful in reproducing measurements of the sediment transport rate (e.g., Bagnold 1956; Berzi & Fraccarollo 2013; Pähtz & Durán 2018, 2020). The reason for the validity of (6.4) is the steady state condition  $u_{fz} = u_{sz} = 0$ , meaning that vertical drag, virtual-mass, and history forces tend to vanish on average. Therefore, among the standard averaged generalized-drag forces, only vertical lift forces can be substantial. However, experimental and numerical measurements of vertical lift forces resulting from the shearing of rough surfaces such as a sediment bed indicate that they tend to be much smaller than streamwise drag forces, except very close to the surface (Chepil 1961; Li *et al.* 2019). Then, in turn, due

to a Coulomb-friction-like law in sediment transport (Pähtz & Durán 2018), the magnitude of streamwise drag forces is comparable to the submerged particle weight, implying that vertical lift forces are also negligible, except close to the bed surface.

Using (3.20), we conclude from (6.3) and (6.4) that

$$\beta_s \langle f_{Bz} \rangle^s \approx -\beta_s \rho_f g_z, \quad (6.5)$$

with the caveat that this relation might be significantly violated close to the bed surface ( $z = 1 \dots 3$ ) due to lift forces.

In figure 4, we compare the predictions of  $\beta_s \langle f_{Bz} \rangle^s$  from our and existing buoyancy closures (Anderson & Jackson 1967; Zhang *et al.* 2007; Chauchat 2018; Maurin *et al.* 2018) with (6.5). It can be seen that our closure and that by Anderson & Jackson (1967) come closest to (6.5), deviating by typically less than 20%, though the latter closure shows larger deviations of about 35% for the lowest-viscosity case,  $\eta_f = 0.001$ . The deviations are almost everywhere to the positive side,  $\beta_s \langle f_{Bz} \rangle^s > -\beta_s \rho_f g_z$ , consistent with the fact that, near the bed surface, lift forces, and therefore the generalized-buoyancy force from (4.14), tend to be positive on average (Chepil 1961; Li *et al.* 2019). It is also noteworthy that these two closures agree especially well with (6.5) in the dilute region of the flow (large  $z$ ) for the turbulent cases  $\eta_f = 0.01$  and  $\eta_f = 0.001$ , whereas the other closures, which do not incorporate the Reynolds stress  $\sigma_{\text{Re}zz}^f$ , persistently deviate in this region. This further supports our conclusion from the thought experiment in §2.1 that the Reynolds stress  $\sigma_{\text{Re}}^f$  fully contributes to the background flow responsible for buoyancy. Furthermore, the closure by Zhang *et al.* (2007) and especially that by Maurin *et al.* (2018) exhibit overall unreasonably strong deviations from (6.5), which supports our conclusion from the thought experiment in §2.2 that the pseudo stress  $\sigma_s^f$ , which is only partially incorporated in these closures, fully contributes to the background flow responsible for buoyancy.

## 7. Summary and Conclusions

In this study, we have revisited an old problem that used to be the matter of debate some decades ago, and which has never been truly resolved ever since: What is the mathematical closure that governs the generalized-buoyancy force density in general disperse two-phase flow? To answer this question, we have exclusively used first-principle-based reasoning: thought experiments for highly idealized, analytically tractable conditions and a rigorous mathematical derivation that can be traced back solely to Newton's axioms. There are no approximations and almost no assumptions involved. The two assumptions needed for our analysis are as follows: (i) a universal buoyancy closure consistent with all possible disperse two-phase flow scenarios does exist, and (ii) this closure can only involve as physical quantities the dispersed-phase volume fraction  $\beta_s$  and the three stresses  $\beta_f \langle \sigma \rangle^f$ ,  $\sigma_{\text{Re}}^f$ , and  $\sigma_s^f$  associated with the fluid phase momentum balance. These stresses emerge from rigorously averaging the fluid's and particles' equations of motion and represent, respectively, the fluid-phase-averaged stress, the Reynolds stress, and the stress due to fluid-particle interactions. They are the only stresses that can conceivably play a role in the problem. From the thought experiments, supported by particle-resolved numerical simulations (§6) and existing experiments (Lamb *et al.* 2017), we have learned that the total effective stress  $\sigma^f \equiv \beta_f \langle \sigma \rangle^f + \sigma_{\text{Re}}^f + \sigma_s^f$  is the only relevant stress in the problem, and that its constituting components  $\beta_f \langle \sigma \rangle^f$ ,  $\sigma_{\text{Re}}^f$ , and  $\sigma_s^f$  should not be looked upon in isolation. This finding then leads to a unique buoyancy closure that depends only on  $\beta_s$  and  $\sigma_s^f$ . It is given by either of the four equivalent expressions (4.7)-(4.10). These expressions involve, in one form or another, the smoothing operator  $\mathcal{L}$  defined in (3.19) and simplified in (4.23) for identically-sized

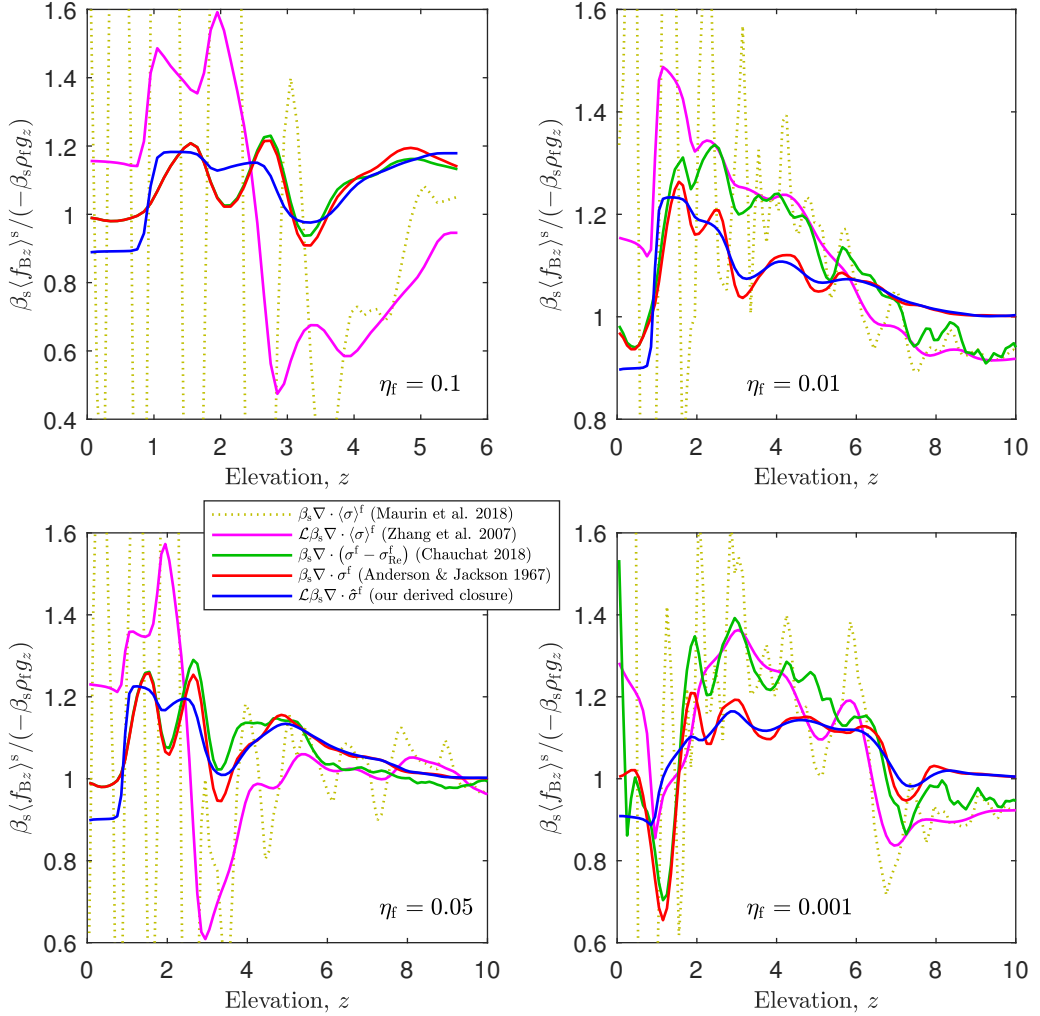


Figure 4: Test of our (4.10) and existing (Anderson & Jackson 1967; Zhang *et al.* 2007; Chauchat 2018; Maurin *et al.* 2018) buoyancy closures against data from DNS-DEM simulations of statistically steady, uniform sediment transport. If lift forces are not significant, one expects  $\beta_s \langle f_{Bz} \rangle^s / (-\beta_s \rho_f g_z) \approx 1$ . However, close to the bed surface ( $z = 1 \dots 3$ ), where significant positive lift forces can occur (Chepil 1961; Li *et al.* 2019), one expects that  $\beta_s \langle f_{Bz} \rangle^s$  is slightly larger than unity. These expectations are met by our closure and that by Anderson & Jackson (1967).

spheres. It essentially represents a low-pass filter, strongly attenuating buoyancy effects at short wavelengths or large wavenumber vectors  $\mathbf{k}$ , asymptotically decaying as  $(R|\mathbf{k}|)^{-4}$ . It is this attenuation effect that prevents buoyancy from causing Hadamard instabilities (§5.1). We have also shown, via generalizing the well-known analysis by Maxey & Riley (1983) for the hydrodynamic force on a submerged sphere at low particle Reynolds numbers (Appendix B), that the virtual-mass force density is suppressed in a similar manner, see (5.14), and that it also does not cause the system of PDEs to become non-hyperbolic.

In conclusion, the ill-posedness problem of two-fluid models (Lhuillier *et al.* 2013), which was linked to the generalized-buoyancy and virtual-mass force densities, was actually never a problem to begin with. It was artificially created by employing mathematical closures for

these densities that do not take into account the particle-size-related smoothing that inherently results from integrating macroscopic quantities such as  $\nabla \cdot \hat{\sigma}^f$  (buoyancy) and  $\mathbf{u}_m$  (virtual mass) over the particles' volumes. For example, when Lhuillier *et al.* (2013) introduced the ill-posedness problem in their review, their very starting point, their equation (2.2), was already inappropriate, and everything that followed was therefore unintentionally about how to treat the symptom rather than the cause.

The expressions derived in this study can be straightforwardly implemented in an approximate manner in numerical two-fluid models, as described in §5.2. In addition, an accurate expression for the generalized-buoyancy force density is a prerequisite for empirically studying two-phase flow rheology with particle-resolved numerical simulations, as we plan to do in the future.

**Acknowledgment.** We acknowledge thought-provoking discussions with Nicolas Fintzi. We thank Jake Langham for discovering a serious mistake in an earlier version of the paper.

**Funding.** Z.H. acknowledges financial support from grant National Key R & D Program of China (2023YFC3008100). R.Z. acknowledges financial support from grant National Natural Science Foundation of China (no. 12402494). T.P. acknowledges financial support from grants National Natural Science Foundation of China (nos. 12350710176, 12272344). Z.H. acknowledges financial support from grant National Natural Science Foundation of China (no. 52171276).

**Declaration of interests.** The authors report no conflict of interest.

## Appendix A. Derivation of $\mathcal{L}$ for a mixture of continuous fluid and identically-sized spheres

Here, we derive an expression for the operator  $\mathcal{L}$  for the case of identically-sized spherical particles of radius  $R$  and volume  $V = 4\pi R^3/3$ . Its definition (3.19) is readily transformed into an expression more suitable for the following analysis:

$$\mathcal{L}\beta_s \mathbf{A} \equiv \beta_s \left\langle \sum_p X^p \underline{\mathbf{A}}_{\mathbb{V}p} \right\rangle^s = \left\langle X_s \sum_p X^p \underline{\mathbf{A}}_{\mathbb{V}p} \right\rangle = \left\langle \sum_p X^p \underline{\mathbf{A}}_{\mathbb{V}p} \right\rangle, \quad (\text{A } 1)$$

where we used (3.5). The goal is now to manipulate  $X^p$  and  $\underline{\mathbf{A}}_{\mathbb{V}p}$  in a manner that allows a straightforward application of the averaging rules in (3.3) and (3.4) afterward. We start the derivation with a general expression for  $\underline{(r_1^p)^k}_{\mathbb{V}p}$ , with  $k \geq 0$  an integer:

$$\underline{(r_1^p)^k}_{\mathbb{V}p} = \frac{3}{4\pi R^3} \int_0^R \int_0^{2\pi} \int_0^\pi (r \cos \theta)^k r^2 \sin \theta d\theta d\phi dr = \frac{3(1 + (-1)^k) R^k}{2(k+1)(k+3)}. \quad (\text{A } 2)$$

Using (A 2) and spherical symmetry, one obtains an expression for  $\underline{\mathbf{A}}_{\mathbb{V}p}$  from the Taylor expansion of  $\mathbf{A}[\mathbf{x}]$  in  $\mathbf{x} = \mathbf{x}^p$ :

$$\mathbf{A}[\mathbf{x}] = \sum_{k=0}^{\infty} \frac{1}{k!} (\mathbf{r}^p[\mathbf{x}])^{(k)} \odot \nabla^{(k)} \mathbf{A}[\mathbf{x}^p] \Rightarrow \underline{\mathbf{A}}_{\mathbb{V}p} = \sum_{k=0}^{\infty} \frac{3R^{2k} \Delta^k \mathbf{A}[\mathbf{x}^p]}{(2k+1)!(2k+3)}, \quad (\text{A } 3)$$

where  $\Delta = \nabla \cdot \nabla$  is the Laplace operator, while  $\cdot^{(k)}$  denotes the  $k$ -th power with respect to the dyadic product (e.g.,  $\mathbf{r}^{(3)} = \mathbf{r}\mathbf{r}\mathbf{r}$ ) and  $\odot$  the full contraction operating as follows:  $\mathbf{A}^{(1)} \odot \mathbf{B}^{(1)} = \mathbf{A} \cdot \mathbf{B}$ ,  $\mathbf{A}^{(2)} \odot \mathbf{B}^{(2)} = \mathbf{A}\mathbf{A} : \mathbf{B}\mathbf{B}$ , and so forth. Defining the differential operator

$$\mathcal{M} \equiv \sum_{k=0}^{\infty} \frac{3R^{2k} \Delta^k}{(2k+1)!(2k+3)}, \quad (\text{A } 4)$$

we can therefore express  $\underline{\mathbf{A}}_{\mathbb{V}p}$  as

$$\underline{\mathbf{A}}_{\mathbb{V}p} = \mathcal{M}\mathbf{A}[\mathbf{x}^p]. \quad (\text{A } 5)$$

The operator  $\mathcal{M}$  also links the indicator function  $X^p$  of a particle  $p$  to the delta distribution  $\delta[\mathbf{x} - \mathbf{x}^p]$  localized in  $\mathbf{x}^p$ :

$$X^p = \mathcal{M}V\delta[\mathbf{x} - \mathbf{x}^p]. \quad (\text{A } 6)$$

This can be readily confirmed through application on a test function  $\phi$  with compact support:

$$X^p[\phi] = \int_{\mathbb{R}^3} X^p \phi d^3x = \int_{\mathbb{V}^p} \phi dV = V\phi_{\mathbb{V}^p}, \quad (\text{A } 7)$$

$$(\mathcal{M}V\delta[\mathbf{x} - \mathbf{x}^p])[\phi] = (V\delta[\mathbf{x} - \mathbf{x}^p])[\mathcal{M}\phi] = V\mathcal{M}\phi[\mathbf{x}^p] = V\phi_{\mathbb{V}^p}. \quad (\text{A } 8)$$

As a consequence of (A 5) and (A 6), the generalized function  $X^p \underline{\mathbf{A}}_{\mathbb{V}^p}$  can be expressed as

$$X^p \underline{\mathbf{A}}_{\mathbb{V}^p} = (\mathcal{M}V\delta[\mathbf{x} - \mathbf{x}^p])(\mathcal{M}\mathbf{A})[\mathbf{x}^p] = \mathcal{M}V\delta[\mathbf{x} - \mathbf{x}^p]\mathcal{M}\mathbf{A}, \quad (\text{A } 9)$$

which again is readily confirmed through application on a test function  $\phi$ :

$$\begin{aligned} (\mathcal{M}V\delta[\mathbf{x} - \mathbf{x}^p])(\mathcal{M}\mathbf{A})[\mathbf{x}^p][\phi] &= (V\delta[\mathbf{x} - \mathbf{x}^p](\mathcal{M}\mathbf{A})[\mathbf{x}^p])[\mathcal{M}\phi] \\ &= (V\delta[\mathbf{x} - \mathbf{x}^p](\mathcal{M}\mathbf{A})[\mathbf{x}])[\mathcal{M}\phi] = (\mathcal{M}V\delta[\mathbf{x} - \mathbf{x}^p]\mathcal{M}\mathbf{A})[\phi]. \end{aligned} \quad (\text{A } 10)$$

Hence, using the averaging rules in (3.3) and (3.4), we obtain

$$\begin{aligned} \mathcal{L}\beta_s \mathbf{A} &= \left\langle \sum_p X^p \underline{\mathbf{A}}_{\mathbb{V}^p} \right\rangle = \left\langle \sum_p \mathcal{M}V\delta[\mathbf{x} - \mathbf{x}^p]\mathcal{M}\mathbf{A} \right\rangle \\ &= \mathcal{M} \left\langle \sum_p V\delta[\mathbf{x} - \mathbf{x}^p]\mathcal{M}\mathbf{A} \right\rangle = \mathcal{M} \left\langle \sum_p V\delta[\mathbf{x} - \mathbf{x}^p] \right\rangle \mathcal{M}\mathbf{A} \\ &= \mathcal{M}nV\mathcal{M}\mathbf{A} = \mathcal{M} \left( \mathcal{M}^{-1}\beta_s \right) \mathcal{M}\mathbf{A}, \end{aligned} \quad (\text{A } 11)$$

where we exploited that  $\mathbf{A}$  is a macroscopic tensor field,  $\mathcal{M}\mathbf{A} = \mathcal{M}\langle \mathbf{A} \rangle = \langle \mathcal{M}\mathbf{A} \rangle$ , and introduced the number density  $n$ , defined as (Pähtz *et al.* 2025)

$$n \equiv \left\langle \sum_p \delta[\mathbf{x} - \mathbf{x}^p] \right\rangle = \mathcal{M}^{-1}\beta_s/V. \quad (\text{A } 12)$$

The equality in (A 12) follows from averaging (A 6).

## Appendix B. Generalization of the analysis by Maxey & Riley (1983) to arbitrary $R/L$

We assume almost the same system as Maxey & Riley (1983): a single rigid sphere of radius  $R$  occupying the domain  $\mathbb{V}$  centered at  $\mathbf{x}_o[t]$  is immersed in an incompressible, Newtonian fluid of density  $\rho_f$  and viscosity  $\eta_f$  that occupies the entire  $\mathbb{R}^3$ . We define the relative flow velocity  $\mathbf{w} = \mathbf{u} - \mathbf{v}_\uparrow$ , where  $\mathbf{v}_\uparrow[t]$  is the sphere's center-of-mass velocity and  $\mathbf{u}[\mathbf{x}, t]$  the actual flow velocity. The velocities  $\mathbf{u}$  and  $\mathbf{w}$  are decomposed into the fields of the undisturbed or background flow, denoted by a tilde, and the disturbance flow, denoted by an asterisk:

$$\mathbf{u} = \tilde{\mathbf{u}} + \mathbf{u}_*, \quad \mathbf{w} = \tilde{\mathbf{w}} + \mathbf{w}_*. \quad (\text{B } 1)$$

The particle Reynolds numbers  $\rho_f \tilde{W}R/\eta_f$  and  $\rho_f \tilde{U}R^2/(\eta_f L)$  are very small, where  $\tilde{W}$  and  $\tilde{U}$  are characteristic background flow velocity scales for  $\tilde{\mathbf{w}}$  and  $\tilde{\mathbf{u}}$ , respectively, and  $L$  the characteristic length scale over which  $\tilde{\mathbf{u}}$  spatially varies. However, in contrast to Maxey & Riley (1983), we do not require  $R/L$  to be small.

Due to the small particle Reynolds numbers,  $\mathbf{w}_*$  satisfies the Stokes equations with the boundary conditions (Maxey & Riley 1983)

$$\mathbf{w}_* = -\tilde{\mathbf{w}} + \omega \times \mathbf{r} \quad \text{for} \quad |\mathbf{r}| = R, \quad (\text{B } 2)$$

$$\mathbf{w}_* = 0 \quad \text{for} \quad |\mathbf{r}| \rightarrow \infty, \quad (\text{B } 3)$$

where  $\omega$  is the sphere's angular velocity and  $\mathbf{r} \equiv \mathbf{x} - \mathbf{x}_o$  the relative coordinate.

Equation (33) of Maxey & Riley (1983) states that the generalized-drag force  $\mathbf{F}_D$  in an arbitrary direction '1' with unit vector  $\mathbf{e}_1$ , in the frequency ( $s$ ) space associated with the Laplace transformation (denoted by an underline), is given by

$$\underline{F}_{D1}[s] = \int_{\partial\mathbb{V}} \mathbf{n} \cdot \underline{\boldsymbol{\sigma}}' \cdot \underline{\mathbf{w}}_* dS + \int_{\mathbb{V}} \rho_f \mathbf{w}_*[\mathbf{x}, 0] \cdot \mathbf{w}'[\mathbf{x}, s] dV_x, \quad (\text{B } 4)$$

where the prime indicates quantities associated with an auxiliary Stokes flow for a sphere with an impulsive velocity  $(\delta[t], 0, 0)$ . The corresponding traction  $\mathbf{n} \cdot \underline{\boldsymbol{\sigma}}'$  is given by equation (38) of Maxey & Riley (1983):

$$\mathbf{n} \cdot \underline{\boldsymbol{\sigma}}' = -\frac{\rho_f s}{2R} \mathbf{e}_1 \cdot \mathbf{r} \mathbf{r} - \frac{3\eta_f}{2R} \left(1 + R\sqrt{\rho_f s/\eta_f}\right) \mathbf{e}_1. \quad (\text{B } 5)$$

Within the surface integral in (B 4), due to the boundary condition (B 2) and spherical symmetry, we can formally replace  $\underline{\mathbf{w}}_*$  by  $-\underline{\tilde{\mathbf{w}}}$ . In addition, by choosing a (somewhat artificial) initial condition where a sphere is introduced to the system just after  $t = 0$  with no slip,  $\mathbf{w}_*[\mathbf{x}, 0] = 0$  for all  $\mathbf{x}$ , the volume integral vanishes and (B 4) simplifies to

$$\underline{F}_{D1} = - \int_{\partial\mathbb{V}} \mathbf{n} \cdot \underline{\boldsymbol{\sigma}}' \cdot \underline{\tilde{\mathbf{w}}} dS. \quad (\text{B } 6)$$

In contrast to Maxey & Riley (1983), we now evaluate (B 6) without approximation. We start with the infinite-order Taylor expansion of  $\underline{\tilde{\mathbf{w}}}[\mathbf{x}]$  in  $\mathbf{x} = \mathbf{x}_o$ :

$$\underline{\tilde{\mathbf{w}}}[\mathbf{x}] = \sum_{k=0}^{\infty} \frac{1}{k!} \mathbf{r}^{(k)} \odot \nabla^{(k)} \underline{\tilde{\mathbf{w}}}[\mathbf{x}_o], \quad (\text{B } 7)$$

whereas Maxey & Riley (1983) stopped the expansion at the second order. The integrals resulting from substituting (B 7) in (B 6) are evaluated in four steps: First, we note that

$$\int_0^{2\pi} \int_0^\pi (R \cos \theta)^k R^2 \sin \theta d\theta d\phi = 4\pi R^2 \frac{(1 + (-1)^k) R^k}{2(k+1)}. \quad (\text{B } 8)$$

Second, introducing the  $k$ -th power of the identity tensor  $\mathbf{1}$  with respect to the tensor product,  $\mathbf{1}^{(k)}$ , e.g.,  $\left(\mathbf{1}^{(2)}\right)_{ijkl} = (\mathbf{1} \otimes \mathbf{1})_{ijkl} = \delta_{ij}\delta_{kl} + \delta_{ik}\delta_{jl} + \delta_{il}\delta_{kj}$ , we can generalize (B 8) to

$$\int_{\partial\mathbb{V}} \mathbf{r}^{(2k)} dS = \frac{4\pi R^{2+2k}}{(2k+1)!!} \mathbf{1}^{(k)}, \quad \int_{\partial\mathbb{V}} \mathbf{r}^{(2k+1)} dS = 0, \quad (\text{B } 9)$$

since the number of distinct permutations of Kronecker delta combinations in  $\mathbf{1}^{(k)}$  is equal to  $(2k-1)!!$ . Third, we note that

$$\mathbf{e}_1 \cdot \left(\mathbf{1}^{(k)} \odot \nabla^{(2k)} \underline{\tilde{\mathbf{w}}}\right) = (2k-1)!! \Delta^k \underline{\tilde{w}}_1, \quad (\text{B } 10)$$

$$\left(\mathbf{e}_1 \cdot \mathbf{1}^{(k+1)}\right) \odot \left(\nabla^{(2k)} \underline{\tilde{\mathbf{w}}}\right) = (2k-1)!! \Delta^k \underline{\tilde{w}}_1, \quad (\text{B } 11)$$

where we used the Laplace-transformed mass balance,  $\nabla \cdot \underline{\tilde{\mathbf{w}}} = 0$ , in (B 11), implying that the result of the contraction of  $\mathbf{e}_1$  with one of the Kronecker deltas in  $\mathbf{1}^{(k+1)}$  must in turn contract with  $\underline{\tilde{\mathbf{w}}}$  to yield a non-vanishing contribution. Fourth, (B 7), (B 9), (B 10), and (B 11) can be

used to calculate:

$$\int_{\partial\mathbb{V}} \mathbf{e}_1 \cdot \underline{\tilde{\mathbf{w}}} dS = \sum_{k=0}^{\infty} \frac{1}{k!} \int_{\partial\mathbb{V}} \mathbf{e}_1 \cdot \left( \mathbf{r}^{(k)} \odot \nabla^{(k)} \underline{\tilde{\mathbf{w}}}[\mathbf{x}_o] \right) dS \quad (\text{B } 12)$$

$$= \sum_{k=0}^{\infty} \frac{4\pi R^{2+2k}}{(2k+1)!} \Delta^k \underline{\tilde{w}}_1[\mathbf{x}_o] \equiv 4\pi R^2 \mathcal{N} \underline{\tilde{w}}_1[\mathbf{x}_o],$$

$$\int_{\partial\mathbb{V}} \mathbf{e}_1 \cdot \mathbf{r} \mathbf{r} \cdot \underline{\tilde{\mathbf{w}}} dS = \sum_{k=0}^{\infty} \frac{1}{k!} \int_{\partial\mathbb{V}} \left( \mathbf{e}_1 \cdot \mathbf{r}^{(k+2)} \right) \odot \left( \nabla^{(k)} \underline{\tilde{\mathbf{w}}}[\mathbf{x}_o] \right) dS \quad (\text{B } 13)$$

$$= \sum_{k=0}^{\infty} \frac{4\pi R^{4+2k}}{(2k+1)!(2k+3)} \Delta^k \underline{\tilde{w}}_1[\mathbf{x}_o] = \frac{4\pi R^4}{3} \mathcal{M} \underline{\tilde{w}}_1[\mathbf{x}_o],$$

where  $\mathcal{N}$  is the surface averaging operator defined as

$$\mathcal{N} \equiv \sum_{k=0}^{\infty} \frac{R^{2k} \Delta^k}{(2k+1)!} \quad (\text{B } 14)$$

or through  $\mathcal{N} \mathbf{A}[\mathbf{x}] = \frac{1}{4\pi R^2} \int_{|\mathbf{r}|=R} \mathbf{A}[\mathbf{x} - \mathbf{r}] dS_{\mathbf{r}}$ . Inserting (B 12) and (B 13) in (B 5) and the result in (B 6), using  $\underline{\tilde{\mathbf{w}}} = \underline{\tilde{\mathbf{u}}} - \mathbf{v}_{\uparrow}$ , yields the generalized-drag force in the frequency space:

$$\underline{\mathbf{F}}_{\text{D}} = 6\pi R \eta_{\text{f}} \left( 1 + R \sqrt{\rho_{\text{f}} s / \eta_{\text{f}}} \right) \left( \mathcal{N} \underline{\tilde{\mathbf{u}}}[\mathbf{x}_o] - \mathbf{v}_{\uparrow} \right) + \frac{2}{3} \pi R^3 \rho_{\text{f}} s \left( \mathcal{M} \underline{\tilde{\mathbf{u}}}[\mathbf{x}_o] - \mathbf{v}_{\uparrow} \right), \quad (\text{B } 15)$$

which is the generalization of equation (40) in Maxey & Riley (1983). The second term on the right-hand side is the Laplace transform of the virtual-mass force  $\mathbf{F}_{\text{VM}}$ , which involves the volume averaging operator  $\mathcal{M}$ . Transforming it back to real space gives

$$\mathbf{F}_{\text{VM}} = \frac{2}{3} \pi R^3 \rho_{\text{f}} \left( \text{d}_t \mathcal{M} \tilde{\mathbf{u}}[\mathbf{x}_o] - \dot{\mathbf{v}}_{\uparrow} \right) \approx \frac{2}{3} \pi R^3 \rho_{\text{f}} \left( \mathcal{M} \tilde{\text{D}}_t \tilde{\mathbf{u}}[\mathbf{x}_o] - \dot{\mathbf{v}}_{\uparrow} \right), \quad (\text{B } 16)$$

where we used  $\text{d}_t \mathcal{M} \tilde{\mathbf{u}}[\mathbf{x}_o] = \mathcal{M}(\partial_t + (\mathbf{v}_{\uparrow} + \boldsymbol{\omega} \times \mathbf{r}) \cdot \nabla) \tilde{\mathbf{u}}[\mathbf{x}_o] \approx \mathcal{M} \tilde{\text{D}}_t \tilde{\mathbf{u}}[\mathbf{x}_o]$  based on Reynolds transport theorem and  $\rho_{\text{f}} \tilde{W} R / \eta_{\text{f}} \ll 1$ .

To translate (B 16) into an expression for the virtual-mass force density  $\beta_{\text{s}} \langle \mathbf{f}_{\text{VM}} \rangle^{\text{s}}$ , we assume a system of spherical particles of constant radius  $R$  and density  $\rho_{\text{s}}$ . In this case, the particle-rotation-free mixture velocity  $\mathbf{u}_{\text{m}} \equiv \langle \mathbf{u}_{\uparrow} \rangle$  is equal to  $\beta_{\text{f}} \mathbf{u}_{\text{f}} + \beta_{\text{s}} \mathbf{u}_{\text{s}}$  and satisfies  $\nabla \cdot \mathbf{u}_{\text{m}} = 0$  (Pähtz *et al.* 2025). The latter property permits identifying the background flow velocity  $\tilde{\mathbf{u}}$  as  $\mathbf{u}_{\text{m}}$  (Fintzi & Pierson 2025). Using (A 11), we can then calculate

$$\begin{aligned} \beta_{\text{s}} \langle \mathbf{f}_{\text{VM}} \rangle^{\text{s}} &\equiv \beta_{\text{s}} \left\langle \sum_p X^p \mathbf{F}_{\text{VM}}^p / V^p \right\rangle^{\text{s}} \approx \frac{\rho_{\text{f}}}{2} \left\langle \sum_p X^p \left( \mathcal{M} \text{D}_t^{\text{m}} \mathbf{u}_{\text{m}}[\mathbf{x}^p] - \dot{\mathbf{v}}_{\uparrow}^p \right) \right\rangle \\ &\approx \frac{\rho_{\text{f}}}{2} \left( \mathcal{L} \beta_{\text{s}} \text{D}_t^{\text{m}} \mathbf{u}_{\text{m}} - \beta_{\text{s}} \text{D}_t^{\text{s}} \mathbf{u}_{\text{s}} \right), \end{aligned} \quad (\text{B } 17)$$

where we evaluated the particle-velocity-related term via (Pähtz *et al.* 2025)

$$\left\langle \sum_p X^p \dot{\mathbf{v}}_{\uparrow}^p \right\rangle = \left\langle \sum_p \left( \partial_t X^p \mathbf{u}_{\uparrow} + \nabla \cdot X^p \mathbf{u} \mathbf{u}_{\uparrow} \right) \right\rangle = \beta_{\text{s}} \left( \partial_t \mathbf{u}_{\text{s}} + \nabla \cdot \langle \mathbf{u}_{\uparrow} \mathbf{u}_{\uparrow} \rangle^{\text{s}} \right) \approx \beta_{\text{s}} \text{D}_t^{\text{s}} \mathbf{u}_{\text{s}}, \quad (\text{B } 18)$$

neglecting the dispersed-phase Reynolds stress  $\boldsymbol{\sigma}_{\text{Re}}^{\text{s}}$  and exploiting the sphericity of the particles via  $\mathbf{u} \cdot \nabla X^p = \mathbf{u}_{\uparrow} \cdot \nabla X^p$ .

- ANDERSON, T. B. & JACKSON, R. 1967 Fluid mechanical description of fluidized beds. Equations of motion. *Industrial & Engineering Chemistry Fundamentals* **6** (4), 527–539.
- BAGNOLD, R. A. 1956 The flow of cohesionless grains in fluid. *Philosophical Transactions of the Royal Society London A* **249** (964), 235–297.
- BATCHELOR, G. K. 2000 *An Introduction to Fluid Dynamics*. Cambridge University Press, Cambridge.
- BERZI, D. & FRACCAROLLO, L. 2013 Inclined, collisional sediment transport. *Physics of Fluids* **25** (10), 106601.
- BIEGERT, E., VOWINCKEL, B. & MEIBURG, E. 2017 A collision model for grain-resolving simulations of flows over dense, mobile, polydisperse granular sediment beds. *Journal of Computational Physics* **340**, 105–127.
- CHASSAGNE, R., BONAMY, C. & CHAUCHAT, J. 2023 A frictional–collisional model for bedload transport based on kinetic theory of granular flows: discrete and continuum approaches. *Journal of Fluid Mechanics* **964**, A27.
- CHAUCHAT, J. 2018 A comprehensive two-phase flow model for unidirectional sheet-flows. *Journal of Hydraulic Research* **56** (1), 15–28.
- CHEPIL, W. S. 1961 The use of spheres to measure lift and drag on wind-eroded soil grains. *Soil Science Society of America Journal* **25** (5), 343–345.
- CLIFT, R., SEVILLE, J. P. K., MOORE, S. C. & CHAVARIE, C. 1987 Comments on buoyancy in fluidised beds. *Chemical Engineering Science* **42** (1), 191–194.
- CROWE, C. T., SCHWARZKOPF, J. D., SOMMERFELD, M. & TSUJI, Y. 2012 *Multiphase Flows with Droplets and Particles*. Taylor & Francis Group, Boca Raton.
- DI FELICE, R. 1995 Hydrodynamics of liquid fluidisation. *Chemical Engineering Science* **50** (8), 1213–1245.
- DREW, D. A. 1983 Mathematical modeling of two-phase flow. *Annual Review of Fluid Mechanics* **15**, 261–291.
- FERZIGER, J. & KAPER, H. 1972 *Mathematical Theory of Transport Processes in Gases*. North-Holland, Amsterdam, The Netherlands.
- FINTZI, N. & PIERSON, J. L. 2025 Averaged equations for disperse two-phase flow with interfacial properties and their closures for dilute suspension of droplets. <https://doi.org/10.48550/arXiv.2410.10752>.
- FOX, R. O. 2019 A kinetic-based hyperbolic two-fluid model for binary hard-sphere mixtures. *Journal of Fluid Mechanics* **877**, 282–329.
- FOX, R. O. 2025 The particle-fluid-particle pressure tensor for ideal-fluid–particle flow. *Journal of Fluid Mechanics* **1010**, A8.
- FRY, B., LACAZE, L., BONOMETTI, T., ELYAKIME, P. & CHARRU, FRANÇOIS 2024 From discrete to continuum description of weakly inertial bedload transport. *Physical Review Fluids* **9** (2), 024304.
- JACKSON, R. 1997 Locally averaged equations of motion for a mixture of identical spherical particles and a Newtonian fluid. *Chemical Engineering Science* **52** (15), 2457–2469.
- JACKSON, R. 2000 *The Dynamics of Fluidized Particles*. Cambridge University Press, New York.
- JAMSHIDI, R. & MAZZEI, L. 2018 CFD modeling of fluidized beds. *Reference Module in Chemistry, Molecular Sciences and Chemical Engineering*.
- JOSEPH, D. D. & SAUT, J. C. 1990 Short-wave instabilities and ill-posed initial-value problems. *Theoretical and Computational Fluid Dynamics* **1**, 191–227.
- KEH, H. J. & CHEN, S. H. 1996 The motion of a slip spherical particle in an arbitrary stokes flow. *European Journal of Mechanics - B/Fluids* **15** (6), 791–807.
- LAMB, MICHAEL P., BRUN, F. & FULLER, B. M. 2017 Direct measurements of lift and drag on shallowly submerged cobbles in steep streams: Implications for flow resistance and sediment transport. *Water Resources Research* **53** (9), 7607–7629.
- LANGHAM, J., MENG, X., WEBB, J. P., JOHNSON, C. G. & GRAY, J.M.N.T. 2025 Ill posedness in shallow multi-phase debris-flow models. *Journal of Fluid Mechanics* **1015**, A52.
- LHUILIER, D., CHANG, C. H. & THEOFANOUS, T. G. 2013 On the quest for a hyperbolic effective-field model of disperse flows. *Journal of Fluid Mechanics* **731**, 184–194.
- LI, X., BALACHANDAR, S., LEE, H. & BAI, B. 2019 Fully resolved simulations of a stationary finite-sized particle in wall turbulence over a rough bed. *Physical Review Fluids* **4** (9), 094302.
- LOTH, E. & DORGAN, A. J. 2009 An equation of motion for particles of finite reynolds number and size. *Environmental Fluid Mechanics* **9**, 187–206.
- MAURIN, R., CHAUCHAT, J. & FREY, P. 2018 Revisiting slope influence in turbulent bedload transport: consequences for vertical flow structure and transport rate scaling. *Journal of Fluid Mechanics* **839**, 135–156.

- MAXEY, M. R. & RILEY, J. J. 1983 Equation of motion for a small rigid sphere in a nonuniform flow. *Physics of Fluids* **26** (4), 883–889.
- PÄHTZ, T., CHEN, Y., RUI, Z., THOLEN, K. & HE, Z. 2025 Coarse-graining particulate two-phase flow. <https://doi.org/10.48550/arXiv.2308.09661>.
- PÄHTZ, T. & DURÁN, O. 2018 Universal friction law at granular solid-gas transition explains scaling of sediment transport load with excess fluid shear stress. *Physical Review Fluids* **3** (10), 104302.
- PÄHTZ, T. & DURÁN, O. 2020 Unification of aeolian and fluvial sediment transport rate from granular physics. *Physical Review Letters* **124** (16), 168001.
- PANICKER, N., PASSALACQUA, A. & FOX, R.O. 2018 On the hyperbolicity of the two-fluid model for gas-liquid bubbly flows. *Applied Mathematical Modelling* **57**, 432–447.
- ROTONDI, M., DI FELICE, R. & PAGLIAI, P. 2015 Validation of fluid–particle interaction force relationships in binary-solid suspensions. *Particuology* **23**, 40–48.
- SHI, P. & RZEHAKE, R. 2019 Lift forces on solid spherical particles in unbounded flows. *Chemical Engineering Science* **208**, 115145.
- STEWART, B. & WENDROFF, B. 1984 Two-phase flow: Models and methods. *Journal of Computational Physics* **56** (3), 363–409.
- THOLEN, K., PÄHTZ, T., KAMATH, S., PARTELI, E. J. R. & KROY, K. 2023 Anomalous scaling of aeolian sand transport reveals coupling to bed rheology. *Physical Review Letters* **130** (5), 058204.
- UHLMANN, M. 2005 An immersed boundary method with direct forcing for the simulation of particulate flows. *Journal of Computational Physics* **209**, 448–476.
- ZHANG, D. Z. 2021 Ensemble average and nearest particle statistics in disperse multiphase flows. *Journal of Fluid Mechanics* **910**, A16.
- ZHANG, D. Z., VANDERHEYDEN, W. B., ZOU, Q. & PADIAL-COLLINS, N. T. 2007 Pressure calculations in disperse and continuous multiphase flows. *International Journal of Multiphase Flow* **33** (1), 86–100.
- ZHU, R., HE, Z., ZHAO, K., VOWINCKEL, B. & MEIBURG, E. 2022 Grain-resolving simulations of submerged cohesive granular collapse. *Journal of Fluid Mechanics* **942**, A49.